

Supplementary Information

Stress response decay with aging visualized using a dual-channel logic-based fluorescent probe

Jingye Tian,^{‡a} Donglei Shi,^{‡b} Yanhui Zhang,^{‡a} Xiaokang Li,^b Xinming Li,^b Hao Teng,^a Tony D. James,^c Jian Li^{*b} and Yuan Guo^{*a}

^aKey Laboratory of Synthetic and Natural Functional Molecule of the Ministry of Education, College of Chemistry and Materials Science, Northwest University, Xi'an, 710127, China.

^bState Key Laboratory of Bioreactor Engineering, Frontiers Science Center for Materiobiology and Dynamic Chemistry, School of Pharmacy, East China University of Science and Technology, 130 Mei Long Road, Shanghai, 200237, China.

^cDepartment of Chemistry, University of Bath, Bath, BA2 7AY, United Kingdom.

[‡]These authors contributed equally to this work.

Email: guoyuan@nwu.edu.cn; jianli@ecust.edu.cn

Table of Contents

1. Materials and general methods.....	S3
2. Spectroscopic properties.....	S7
3. Cytotoxicity studies	S14
4. Images of compounds.....	S15
5. Confocal imaging	S15
6. Synthetic methods	S17
7. Characterization of compounds.....	S22
References	S35

1. Materials and general methods

Unless specifically stated, all chemical reagents were used of the highest available quality and were used directly without further purification or distillation. XL413 was purchased from MedChemExpress (USA). All solvents and inorganic salts were analytical grade unless otherwise noted. Distilled water was used for all experiments. Analytical thin-layer chromatography (TLC) used commercial silica gel plates (GF254). Flash column chromatography was performed using Merck silica gel (200-300 mesh). The composition of mixed solvents is given by the volume ratio (v/v). The ^1H NMR and ^{13}C NMR spectra were acquired on a Varian Unity INOVA-400 spectrometer, Bruker 400, Bruker 600 instruments and JEOL spectrometer operating at 400 MHz. High-resolution mass spectra (HRMS) were performed with a Bruker micro-TOF-QII mass spectrometer (Bruker Daltonics Corp, Germany) in electrospray ionization (ESI) mode. The single crystal structures were determined by X-ray crystallography with a Bruker SMART APEX-CCD system and a Bruker VEBTURE system. The pictures of solid powders were taken on Nikon SMZ18 solid microscope. Absolute fluorescence quantum yields were measured using the Absolute PL quantum yield spectrometer C9920-02G (Hamamatsu). The pH measurements were carried out on a Mettler Toledo pH meter. The refractive indices were measured using the abbe refractometer (INESA WYA, China). The fluorescence spectra were measured with a Hitachi F-2700 fluorescence spectrophotometer (Tokyo, Japan) with a 10 mm quartz cuvette. The UV-visible absorption spectra were determined by a MAPADA UV-1800 spectrophotometer with a 10 mm quartz cuvette. Fluorescence imaging studies of cells were observed using a confocal laser scanning microscope (Nikon A1plus, Japan) with excitation wavelength at 488 nm and 561 nm. Fluorescence imaging studies of *C. elegans* were recorded using a confocal laser scanning microscope (Leica TCS SP8) with excitation wavelength at 488 nm and 561 nm.

X-ray crystallography details

The single crystal of **ROB** was obtained by diffusion method and the crystal was purple and transparent. The single crystals of **ROCL**, **ROCZ** and **ROE** were grown from a mixture of ethanol and dichloromethane by volatilization method and the crystals were colourless and transparent. The single crystals of **ROKS** and **ROZ** were obtained by diffusion method and the crystals were yellow and transparent. Single-crystal X-ray experiments were performed using a Bruker Smart Apex CCD diffractometer equipped with a graphite-monochromatized Mo K α radiation ($\lambda = 0.71073 \text{ \AA}$) using ω and ϕ scan mode at room temperature and a Bruker VENTURE system with a Ga-target liquid METALJET D2 PLUS X-ray Source ($\lambda = 1.34139 \text{ \AA}$) at 174K. The data integration and reduction were processed with SAINT software. The structures were solved by the direct method using SHELXS and refined by a full-matrix least-

squares method on F2 with the SHELXL-2014 program.^{1,2} Hydrogen atoms were placed in geometrically calculated positions. A summary of the crystallographic data and the structure refinement parameters of **ROB**, **ROCL**, **ROCZ**, **ROE**, **ROKS** and **ROZ** are given in Table S2-S3, respectively. The crystallographic data for **ROB**, **ROCL**, **ROCZ**, **ROE**, **ROKS** and **ROZ** can be found in the CCDC with the numbers 2018837, 2018838, 2018841, 2018842, 2018843 and 2018844.

Preparation of UV-Vis and fluorescence spectral measurements

ROKS, **ROCL**, **ROB**, **ROE**, **ROCZ** and **ROZ** were dissolved in analytical grade DMF to obtain stock solutions (1 mM), respectively. The stock solution of thiophenol (10 mM) were prepared in analytical grade DMF. The stock solution of various ROS including HOCl, O₂⁻, NO[•], TBHP, H₂O₂, [•]OH, ¹O₂, TBO[•] and ONOO⁻ were prepared according to previous reports.^{3,4} The stock solutions of various ions (1 mM) including Fe³⁺, Al³⁺, Zn²⁺, Mg²⁺, HSO₃⁻, HSO₄⁻, S₂O₃²⁻, SCN⁻, NO₂⁻, NO₃⁻, HCO₃⁻, CO₃²⁻, F⁻, Cl⁻, Br⁻ and I⁻ were prepared by direct dissolution of corresponding salt in distilled water. Small biological molecules (Cys, Hcy and GSH) were dissolved in distilled water to obtain stock solutions (1 mM).

Measurement of relative fluorescence quantum yields

The relative fluorescence quantum yield of compound **ROB** was determined in PBS buffer solution (10 mM, pH = 7.4, containing 10% DMF) using Rhodamine B as a reference with a known Φ value of 0.89 in ethylene glycol excited at 535 nm.⁵ The relative fluorescence quantum yields of compounds **ROCL**, **ROCZ** and **ROE** were determined in PBS buffer solution (10 mM, pH = 7.4, containing 10% DMF) using quinine sulfate as a reference with a known Φ value of 0.55 in 0.1 M H₂SO₄ excited at 365 nm.⁶ The relative fluorescence quantum yields of compounds were calculated following the equation (1):

$$\Phi_S/\Phi_R = (F_S/F_R) \times (A_R/A_S) \times (\eta_S^2/\eta_R^2) \quad (1)$$

Where *S* and *R* are the sample and the reference, respectively. Φ is the fluorescence quantum yield. *F* is the relative integrated fluorescence emission area. *A* is the absorbance at the excitation wavelength. η is the refractive index of the solvent. The refractive indices of ethylene glycol, H₂SO₄ (0.1 M) and PBS buffer solution (10 mM, pH = 7.4, containing 10% DMF) were measured respectively to be 1.4274, 1.3335 and 1.3463 by abbe refractometer (INESA WYA, China).

Measurement of absolute fluorescence quantum yields

The absolute fluorescence quantum yields of compounds in solid form were determined by the Absolute PL quantum yield spectrometer C9920-02G.

Determination of detection limit

The limit of detection (LOD) was determined from the fluorescence titration data. According to the results of the titrating experiment, a good linear relationship between the fluorescence intensity and the determinand concentration was obtained. The detection limit was calculated by means of equation (2):

$$\text{LOD} = 3\sigma/K \quad (2)$$

Where σ is the standard deviation of the blank measurement and K is the slope of the calibration curve.

Density functional theory calculations

Gaussian 09 program at ω B97X-D/6-31G(d,p) level of theory was employed to optimize the ground state (GS) of 1,3-dinitrobenzene and the triplet state of **ROCL**, and then the orbital energies were calculated.^{7,8} To mimic the d-PeT process, 1,3-dinitrobenzene was calculated using the GS where the LUMO orbital was occupied by an electron pair. However, **ROCL** was calculated using the triplet state in which each HOMO and LUMO were occupied by a single electron, respectively.

Cell culture

The HepG2 cells line were obtained from Procell Life Science & Technology Co., Ltd (Wuhan, China). The HepG2 cells were cultured in Dulbecco's modified Eagle's medium (DMEM) containing 10% fetal bovine serum (FBS). The HepG2 cells were seeded at a density of 1×10^5 cells per dish and cultured in a humidified atmosphere of 5% CO₂ and 95% air at 37 °C. For senescence induction, HepG2 cells were supplemented with media including XL413 (5 μ M) for different times (3 days and 5 days). For cell fixation, HepG2 cells were added with 4% paraformaldehyde and incubated for 10 min.

Cytotoxicity assay

The cytotoxicity of **ROKS** to HepG2, MRC-5, HL-7702, Hela and A549 cells and **ROCL** to HepG2 cells was assessed by performing standard Cell Counting Kit-8 (CCK-8) assay.⁹ cells (5×10^3 cells/well) were seeded into 96-well plates in DMEM medium containing 10% FBS and cultured at 37 °C under 5% CO₂ for 24 h. Different concentrations of **ROKS** and **ROCL** (0, 10, 20, 30, 40 and 50 μ M) were added to the wells. After incubation for 24 h, 100 μ L CCK-8 solution (10% in serum free culture medium) was added to each well, and the plate was incubated for another 2 h. The absorbance of each well at 450 nm were measured by a microplate reader, and then the viability of cells was calculated using equation (3):

$$\text{cell viability} = (\text{OD}_{\text{positive}} - \text{OD}_{\text{control}}) / (\text{OD}_{\text{negative}} - \text{OD}_{\text{control}}) \quad (3)$$

Western blot analysis

HepG2 cells were incubated with XL413 (5 μ M) under 5% CO₂ in air and humidified atmosphere at 37 °C for 3 days. Then the XL413-incubated cells were washed with PBS three times, removed from plates and dipped in RIPA buffer that contain protease inhibitor. The concentration of proteins was determined using a BCA proteins assay kit. Protein samples were mixed with SDS-PAGE loading buffer and were heated for 10 min at 100 °C to fully denature the proteins. A 10% SDS-PAGE gel was used to separate the proteins, followed by transfer onto a PVDF membrane at 300 mA for 2 h to measure the expression level of the targeted proteins. 5 % skim milk in 0.1% tris buffered/tween 20 (TBST) were utilized to block membrane for one hour at room temperature and the membrane were incubated along with antibodies (γ -H2AX: Abcam, ab81299, 1/10000 dilution; GAPDH: Abclonal, ac033, 1/2000 dilution) at 4 °C for 12 h. Finally, the membrane was washed with TBST and further incubated with secondary antibodies (Anti-rabbit IgG antibody, CST, 7074P2; Goat anti-Mouse IgG antibody, Arigo, ARG65350) for 1 h and then chemiluminescence enhancement method was used to check protein's signal. Tanon-4600SF image-capturing system was utilized to image the gels.

X-gal staining assay

X-gal staining was performed according to the X-gal staining kit protocols (Beyotime Biotechnology). The HepG2 cells pre-incubated with XL413 (5 μ M) for 5 days were cultured at 37 °C and then fixed with 4% paraformaldehyde for 10 min. Subsequently, the HepG2 cells were treated with X-gal solution (1 mg/mL) and cultured at 37 °C overnight. After that, the HepG2 cells were washed by PBS buffer solution for three times and the change of blue color was observed under an inverted microscope.

***C. elegans* culture and imaging**

C. elegans were grown and maintained on nematode growth medium (NGM) agar plates at 20 °C. They were fed *Escherichia coli* strain OP50 (*Escherichia coli*) and cultured under standard conditions until the worms reached the young adult, then picked the worms which were cultured for 6 days and 12 days to the next experiment. The *C. elegans* were incubated with **ROKS** (30 μ M) in centrifuge tubes for 60min and treated with PhSH (3 μ M) for different times (0, 15, 30, 45 and 60 min), then picked for imaging.

2. Spectroscopic properties

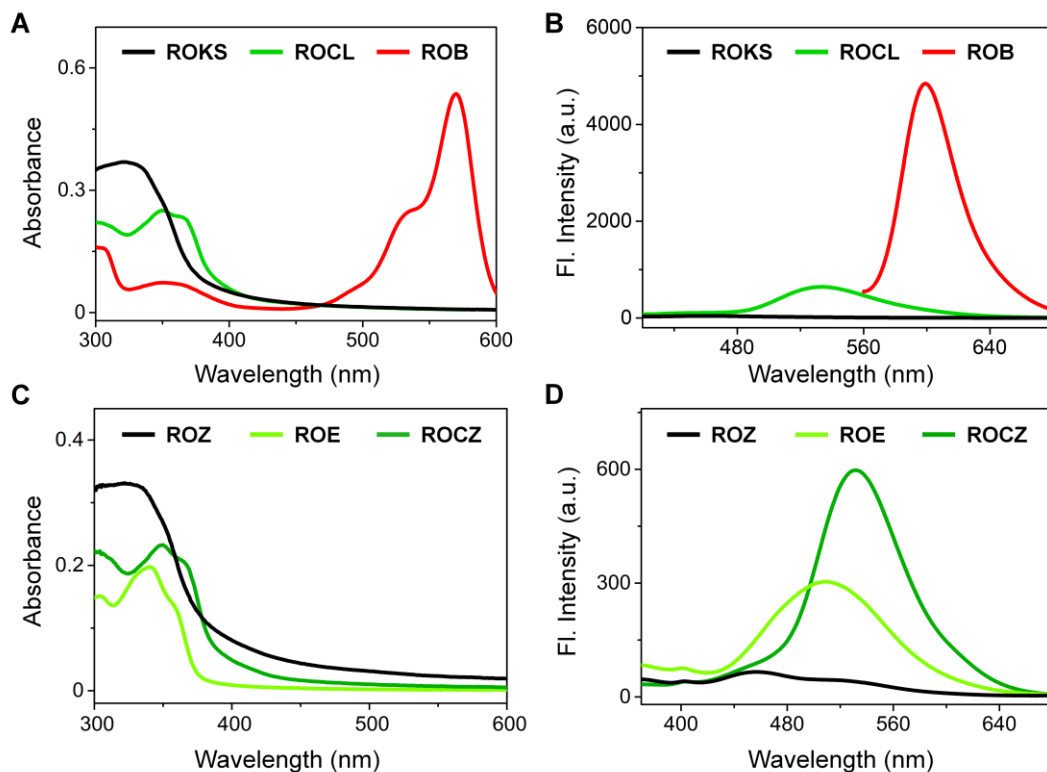


Figure S1. (A-B) Absorption (A) and fluorescence spectra (B) of **ROKS**, **ROCL** and **ROB** in PBS buffer solution (10 mM, pH = 7.4, containing 10% DMF). (C-D) Absorption (C) and fluorescence spectra (D) of **ROZ**, **ROE** and **ROCZ** in PBS buffer solution (10 mM, pH = 7.4, containing 10% DMF). $\lambda_{\text{ex}} = 350$ nm for **ROKS**, **ROCL**, **ROZ**, **ROE** and **ROCZ**; $\lambda_{\text{ex}} = 550$ nm for **ROB**, slit widths: 2.5 nm/5.0 nm.

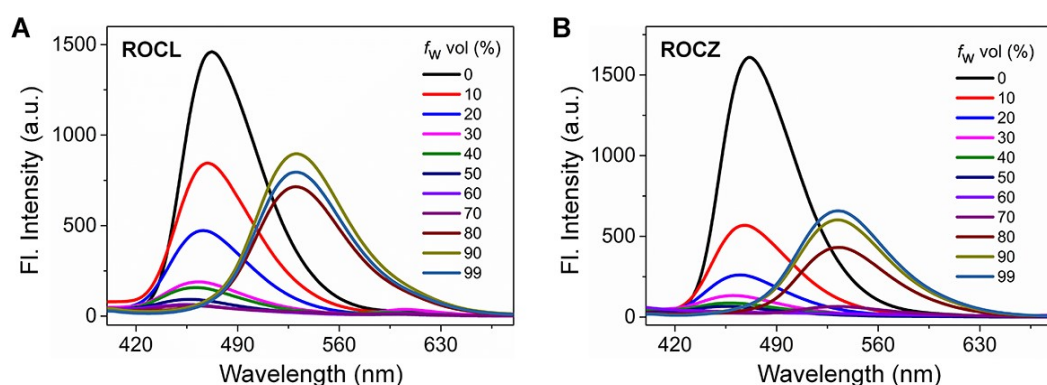


Figure S2. (A) Fluorescence spectra of **ROCL** (10 μM) in a mixture of DMF and water with diverse water fractions (f_w). (B) Fluorescence spectra of **ROCZ** (10 μM) in a mixture of DMF and water with diverse water fractions (f_w). $\lambda_{\text{ex}} = 350$ nm, slit widths: 2.5 nm/5.0 nm.

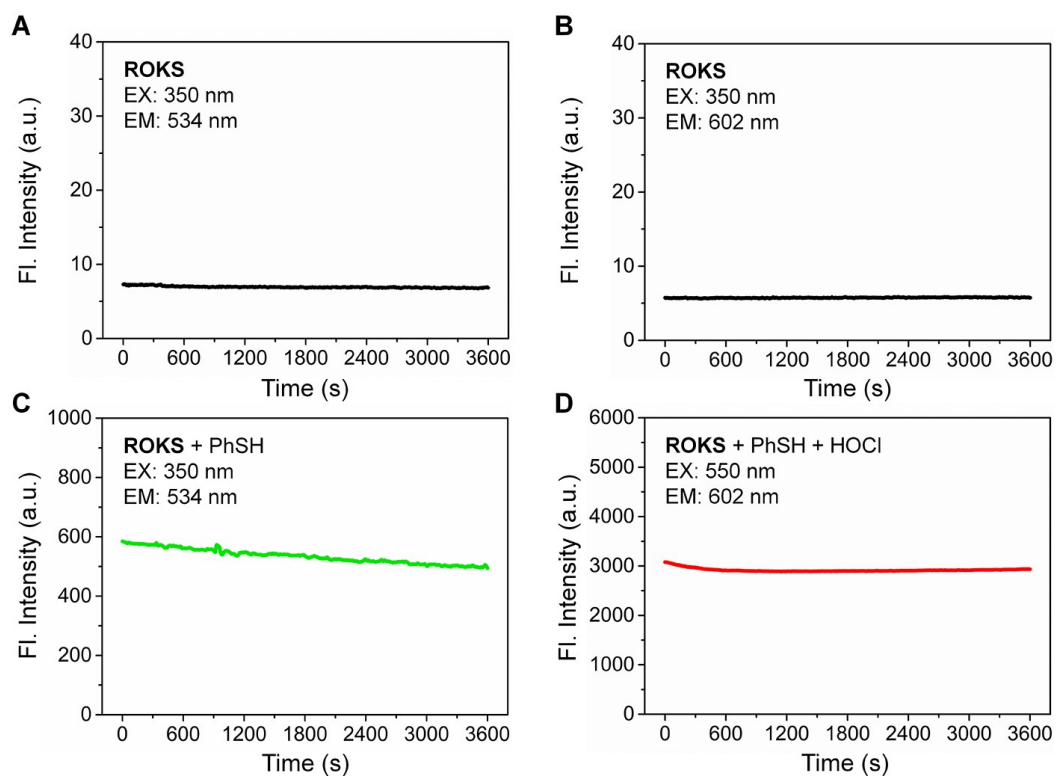


Figure S3. Photostability profiles of **ROKS** (10 μ M) (A-B), **ROKS** (10 μ M) upon addition of PhSH (200 μ M, 11 min) (C) and **ROKS** (10 μ M) upon addition of PhSH (200 μ M, 11 min) followed by HOCl (100 μ M, 30 s) (D) in PBS buffer solution (10 mM, pH = 7.4, containing 10% DMF). Slit widths: 2.5 nm/5.0 nm.

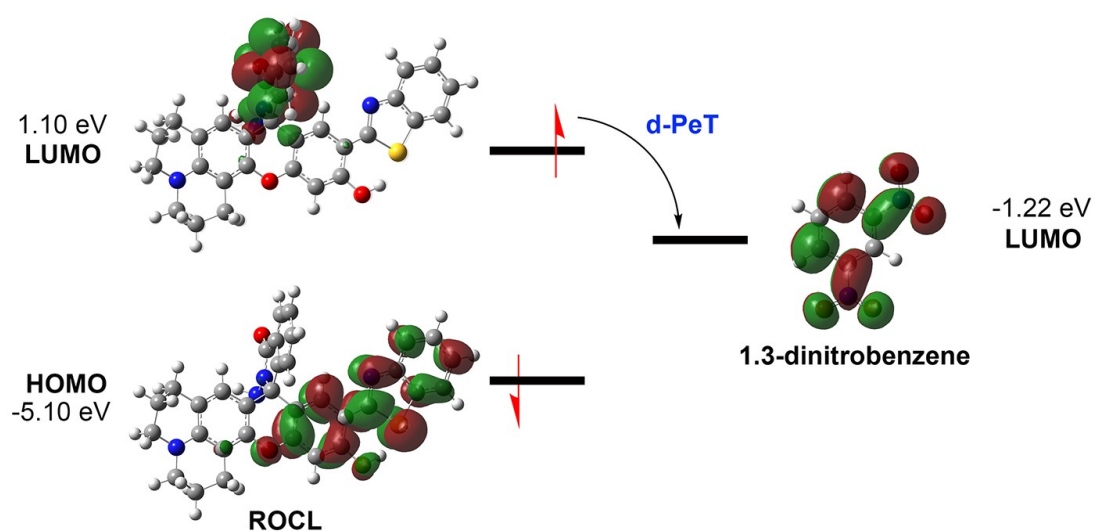
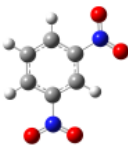
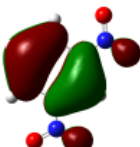
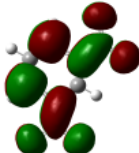
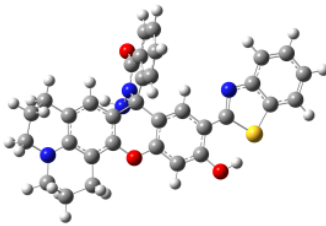
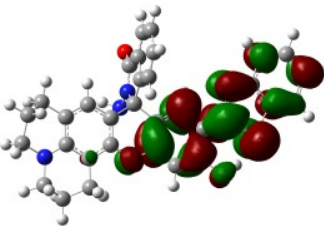
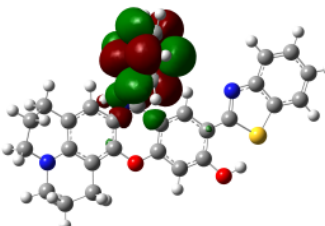


Figure S4. Frontier orbital energy diagram. Illustration of the thermodynamic simulation of the fluorescence OFF/ON switch by the d-Pet process.

Table S1. The calculated HOMO-LUMO orbital energies of the 1,3-dinitrobenzene and ROCL.

Compound	HOMO (eV) ^a	LUMO (eV) ^a
 1,3-dinitrobenzene (GS) ^b	 (-10.51)	 (-1.22)
 ROCL(trp) ^c	 (-5.10)	 (1.10)

^a Orbital energies (in eV) were calculated at the B3LYP/6-31G level of theory.

^b “GS” denotes the compound calculated in ground state.

^c “triplet” denotes the compound calculated in triplet state.

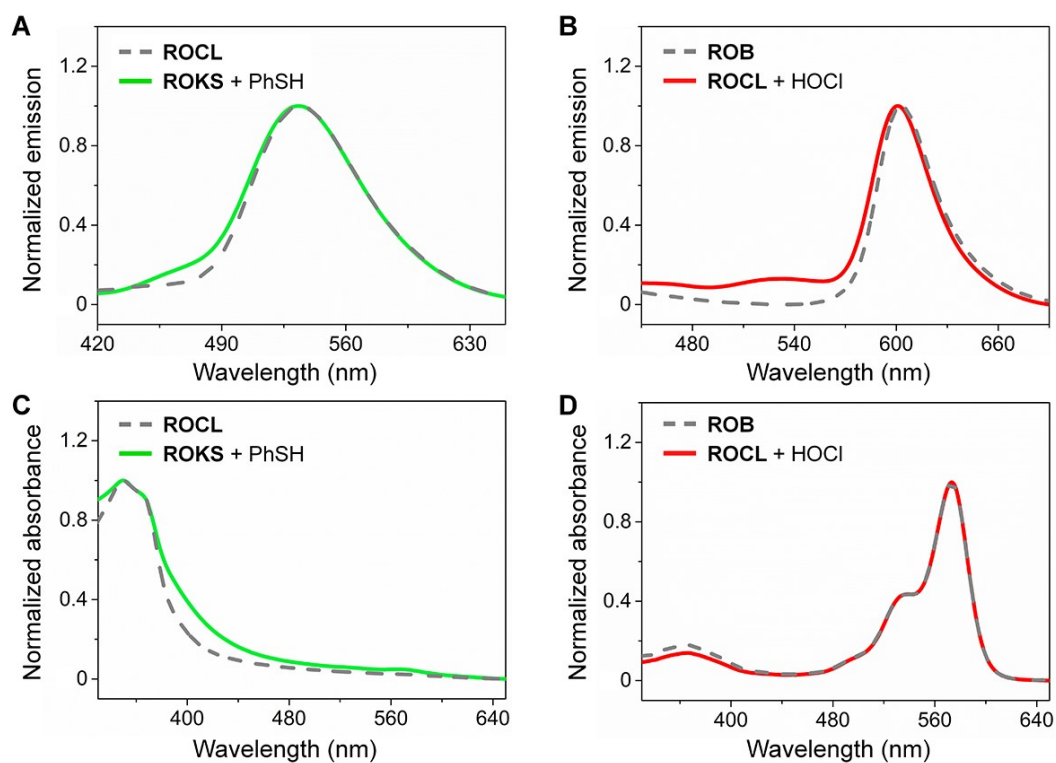


Figure S5. (A) Normalized emission spectra of **ROCL** and the reaction system of **ROKS** with PhSH in PBS buffer solution (10 mM, pH = 7.4, containing 10% DMF). (B) Normalized emission spectra of **ROB** and the reaction system of **ROCL** with HOCl in PBS buffer solution (10 mM, pH = 7.4, containing 10% DMF). $\lambda_{\text{ex}} = 350$ nm, slit widths: 2.5 nm/5.0 nm. (C) Normalized absorbance spectra of **ROCL** and the reaction system of **ROKS** with PhSH in PBS buffer solution (10 mM, pH = 7.4, containing 10% DMF). (D) Normalized absorbance spectra of **ROB** and the reaction system of **ROCL** with HOCl in PBS buffer solution (10 mM, pH = 7.4, containing 10% DMF).

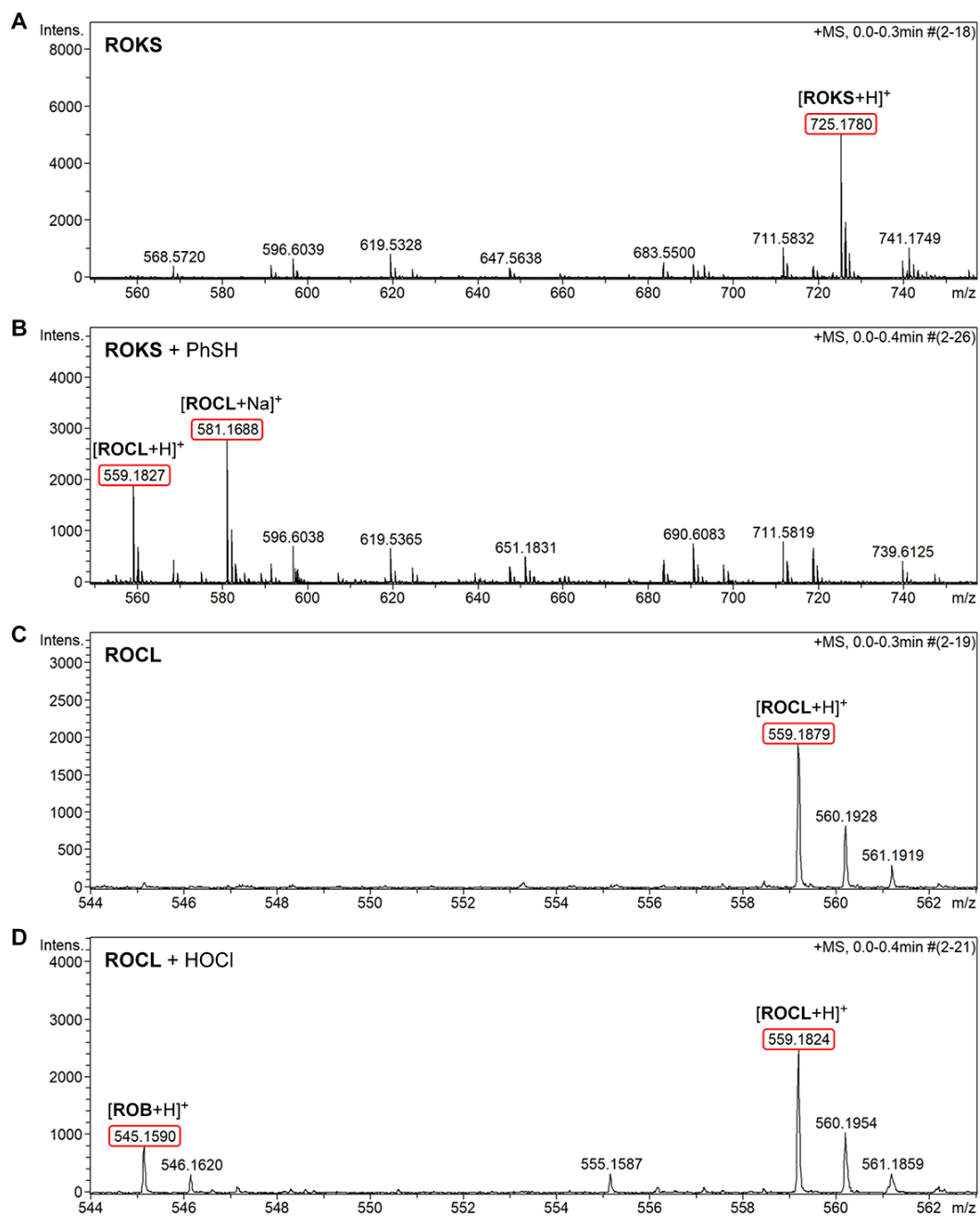


Figure S6. (A) HRMS spectra of **ROKS** in methanol. (B) HRMS spectra of reaction product of **ROKS** with PhSH in methanol. (C) HRMS spectra of **ROCL** in methanol. (D) HRMS spectra of reaction product of **ROCL** with HOCl in methanol.

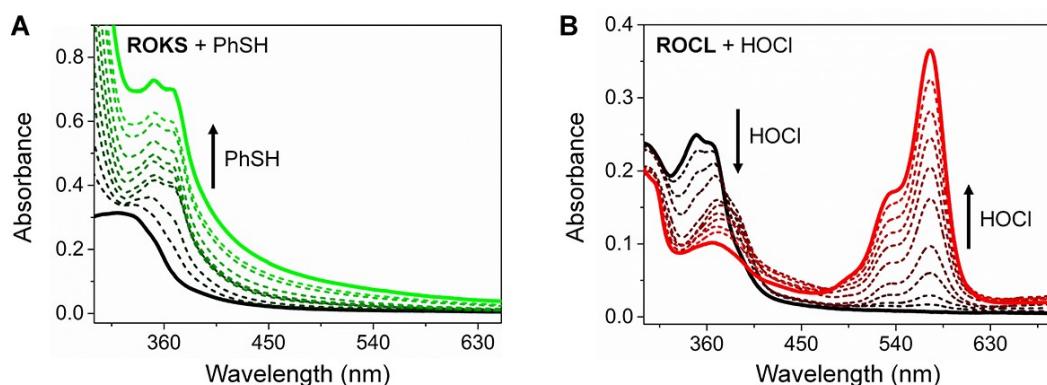


Figure S7. (A) Absorption spectra of **ROKS** (10 μ M) upon addition of PhSH (0-200 μ M) in PBS bufer solution (10 mM, pH = 7.4, containing 10% DMF). (B) Absorption spectra of **ROCL** (10 μ M) upon addition of HOCl (0-100 μ M) in PBS bufer solution (10 mM, pH = 7.4, containing 10% DMF).

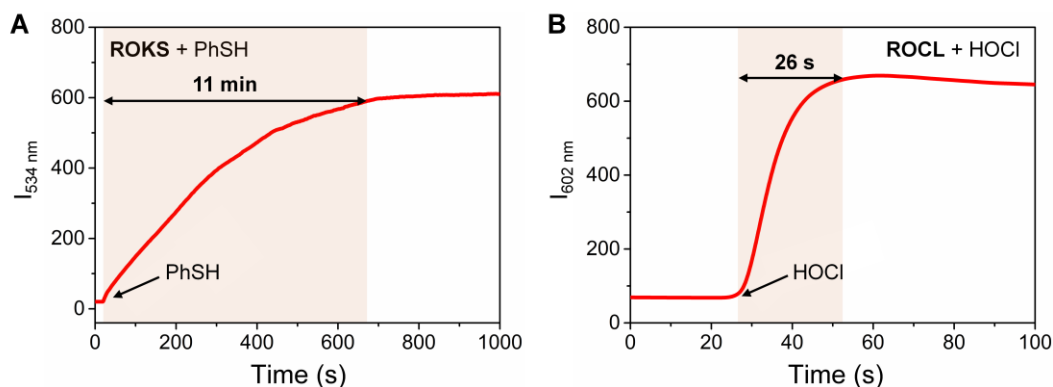


Figure S8. (A) Time-course fluorescence spectra of **ROKS** (10 μ M) in the presence of PhSH (200 μ M) in PBS buffer solution (10 mM, pH = 7.4, containing 10% DMF). (B) Time-course fluorescence spectra of **ROCL** (10 μ M) in the presence of HOCl (40 μ M) in PBS buffer solution (10 mM, pH = 7.4, containing 10% DMF). λ_{ex} = 350 nm, slit widths: 2.5 nm/5.0 nm.

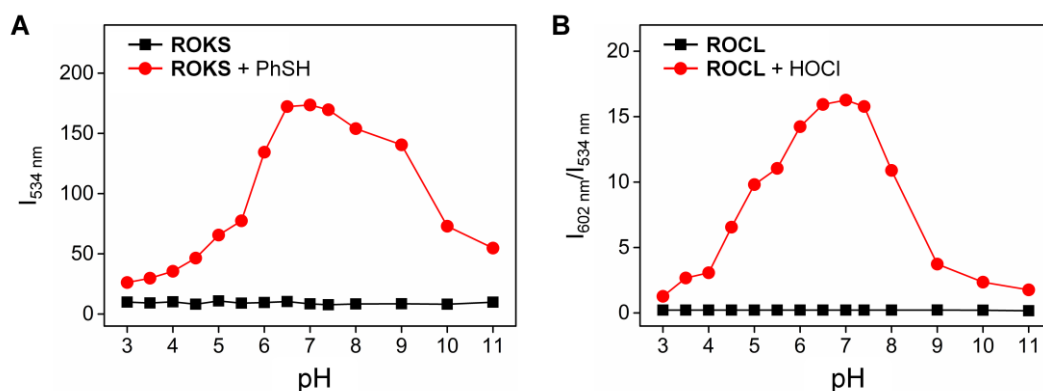


Figure S9. (A) Fluorescence spectra of **ROKS** (10 μ M) in the absence (black) and presence (red) of PhSH (50 μ M) at various pH values in PBS buffer solutions (10 mM, containing 10%

DMF). (B) Fluorescence spectra of **ROCL** (10 μ M) in the absence (black) and presence (red) of HOCl (40 μ M) at various pH values in PBS buffer solutions (10 mM, containing 10% DMF). λ_{ex} = 350 nm, slit widths: 2.5 nm/5.0 nm.

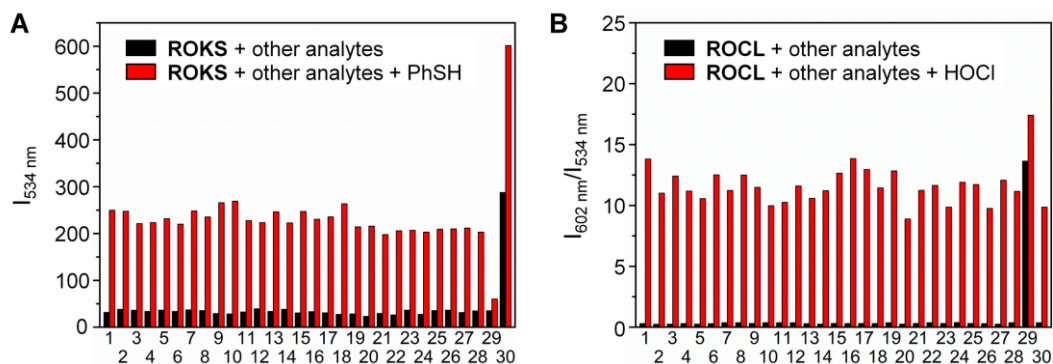


Figure S10. (A) Selectivity and competition response of **ROKS** (10 μ M) to PhSH (100 μ M) against GSH (1 mM) or other analytes (100 μ M) in PBS buffer solution (10 mM, pH = 7.4, containing 10% DMF). (B) Selectivity and competition response of **ROCL** (10 μ M) to HOCl (40 μ M) against GSH (1 mM) or other analytes (40 μ M) in PBS buffer solution (10 mM, pH = 7.4, containing 10% DMF). λ_{ex} = 350 nm, slit widths: 2.5 nm/5.0 nm. (1. Blank, 2. Fe^{3+} , 3. Al^{3+} , 4. Zn^{2+} , 5. Mg^{2+} , 6. HSO_3^- , 7. HSO_4^- , 8. $\text{S}_2\text{O}_3^{2-}$, 9. SCN^- , 10. NO_2^- , 11. NO_3^- , 12. HCO_3^- , 13. CO_3^{2-} , 14. F^- , 15. Cl^- , 16. Br^- , 17. I^- , 18. Cys, 19. Hcy, 20. GSH, 21. H_2O_2 , 22. $\cdot\text{OH}$, 23. O_2^- , 24. $^1\text{O}_2$, 25. $\text{NO}\cdot$, 26. $\text{TBO}\cdot$, 27. TBHP, 28. ONOO^- , 29. HOCl, 30. PhSH).

3. Cytotoxicity studies

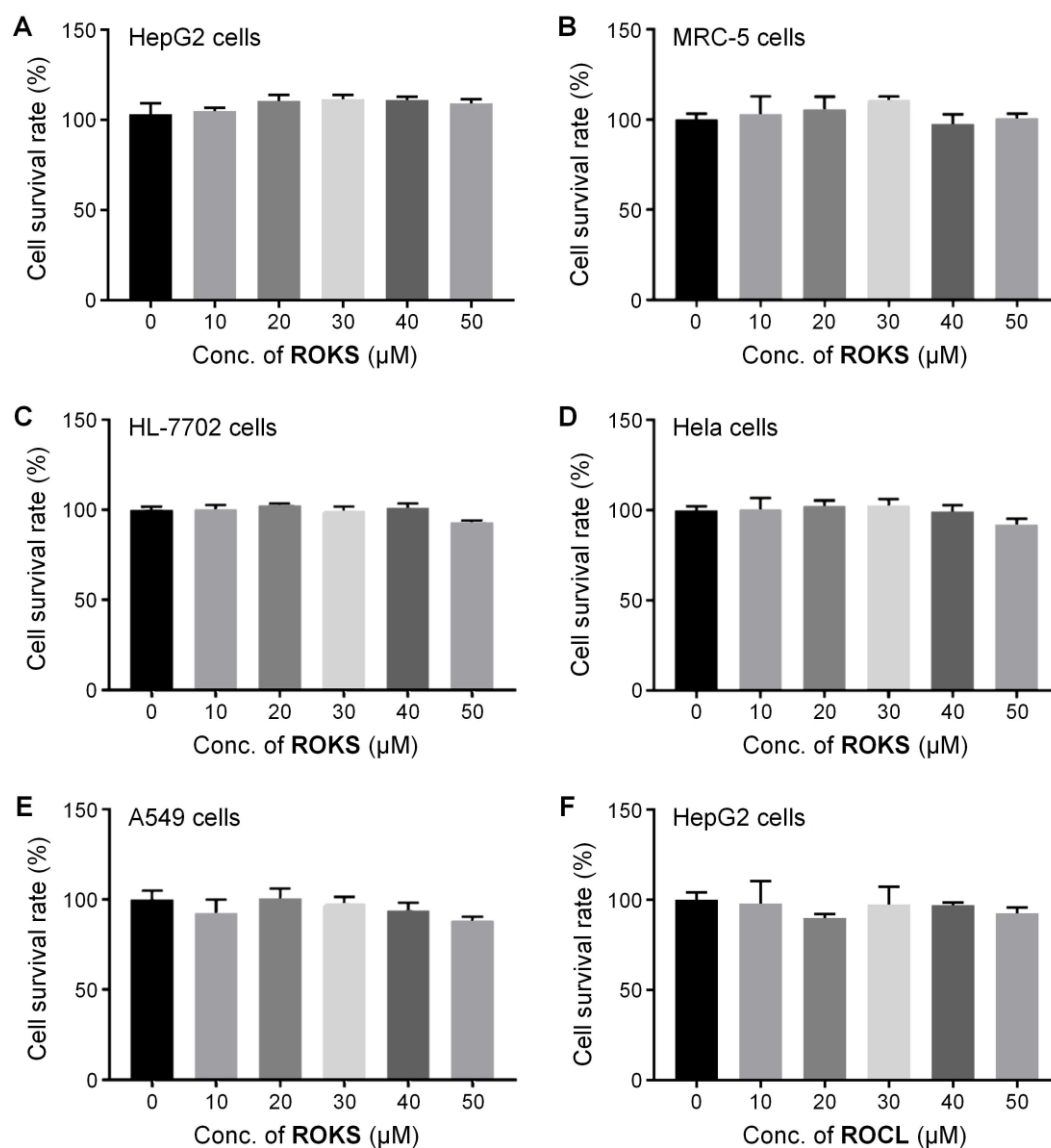


Figure S11. (A-E) Survival rate of HepG2 cells (A), MRC-5 cells (B), HL-7702 cells (C), Hela cells (D) and A549 cells (E) treated with different concentrations of **ROKS** for 24 h. (F) Survival rate of HepG2 cells treated with different concentrations of **ROCL** for 24 h. Cell survival rate was assayed by the CCK-8 method (values: mean \pm standard deviation). Error bars are represented as the standard deviation (\pm S.D.) with $n = 5$.

4. Images of compounds

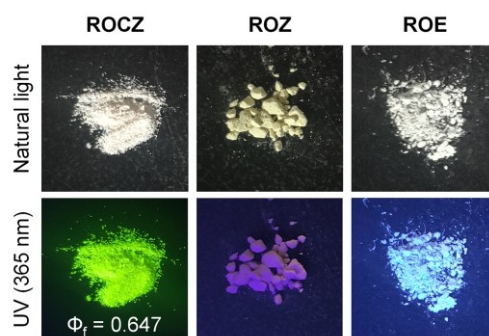


Figure S12. Images of **ROCZ**, **ROZ** and **ROE** in solid state under natural light and UV light of 365 nm, respectively.

5. Confocal imaging

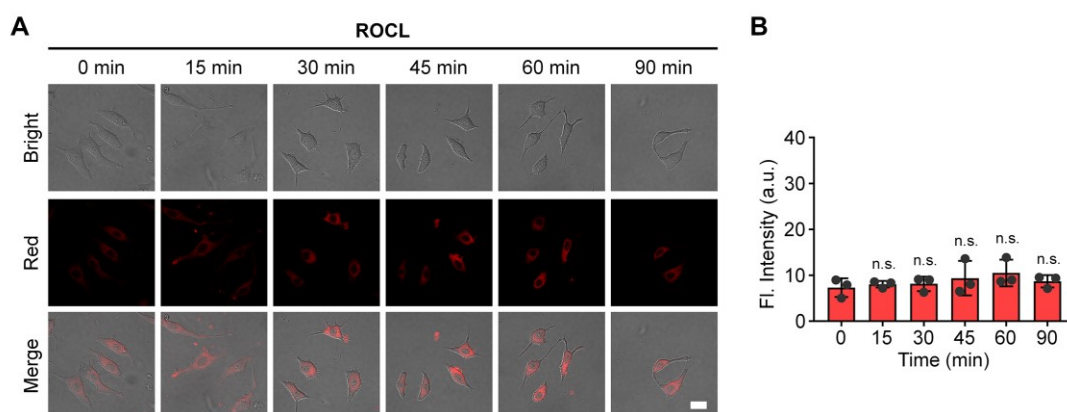


Figure S13. (A) Representative confocal fluorescence images from HepG2 cells treated with **ROCL** (30 μ M, 30 min) and then imaged at different times (0, 15, 30, 45, 60 and 90 min). (B) Average fluorescence intensity in the red channel from parallel images including (A). Scale bar: 25 μ m. Red channel for HOCl: $\lambda_{\text{ex}} = 561$ nm, $\lambda_{\text{em}} = 570\text{--}620$ nm. Error bars are represented as the standard deviation (\pm S.D.) with $n = 3$. The number of dots represents that of samples. Significant differences (n.s., not significant) are analyzed with two-sided Student's t-test.

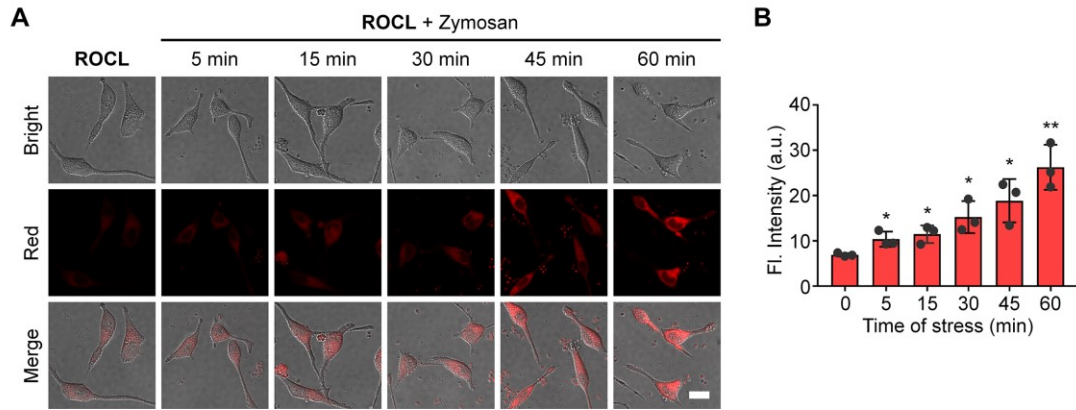


Figure S14. (A) Representative confocal fluorescence images from HepG2 cells treated with **ROCL** (30 μ M, 30 min) and then stimulated with zymosan (10 μ g/mL) for different times (0, 5, 15, 30, 45 and 60 min). (B) Average fluorescence intensity in the red channel from parallel images including (A). Scale bar: 20 μ m. Red channel for HOCl: λ_{ex} = 561 nm, λ_{em} = 570-620 nm. Error bars are represented as the standard deviation (\pm S.D.) with n = 3. The number of dots represents that of samples. Significant differences (* P < 0.05, ** P < 0.01) are analyzed with two-sided Student's t-test.

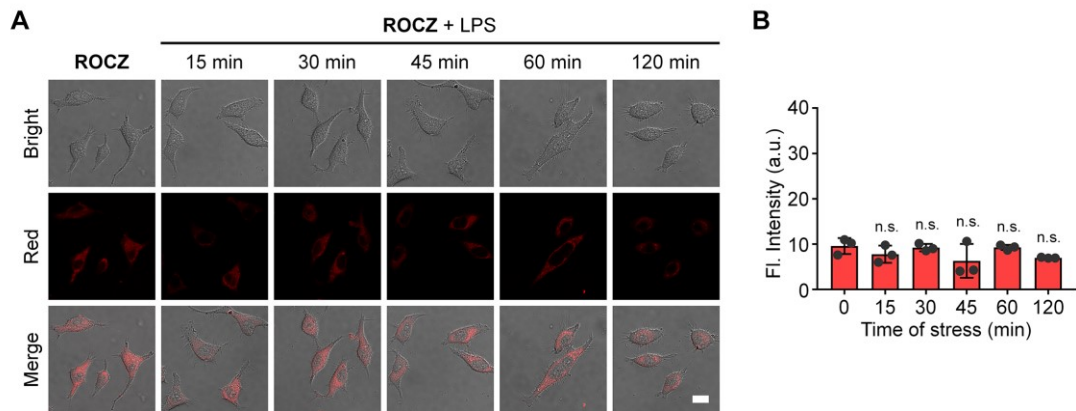


Figure S15. (A) Representative confocal fluorescence images from HepG2 cells treated with **ROCZ** (30 μ M, 30 min) and then stimulated with LPS (10 μ g/mL) for different times (0, 15, 30, 45, 60 and 120 min). (B) Average fluorescence intensity in the red channel from parallel images including (A). Scale bar: 25 μ m. Red channel for HOCl: λ_{ex} = 561 nm, λ_{em} = 570-620 nm. Error bars are represented as the standard deviation (\pm S.D.) with n = 3. The number of dots represents that of samples. Significant differences (n.s., not significant) are analyzed with two-sided Student's t-test.

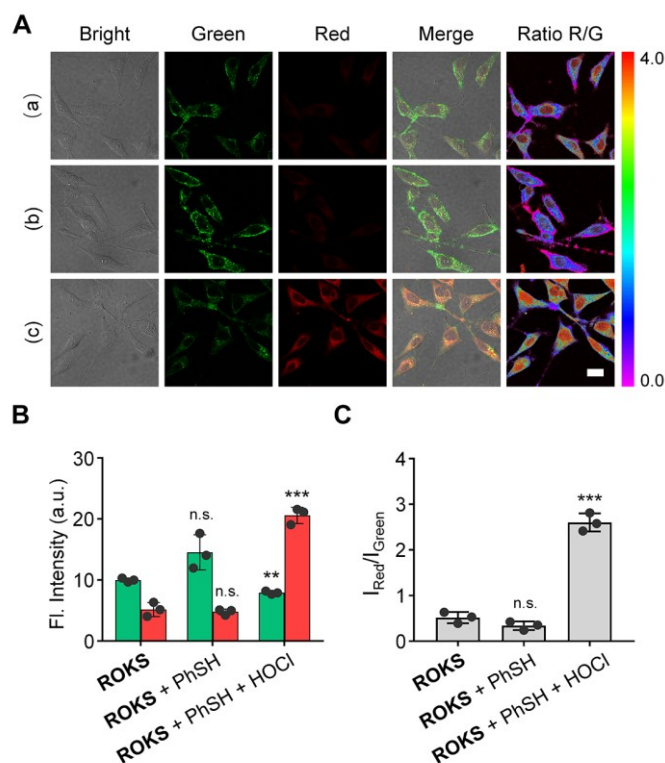
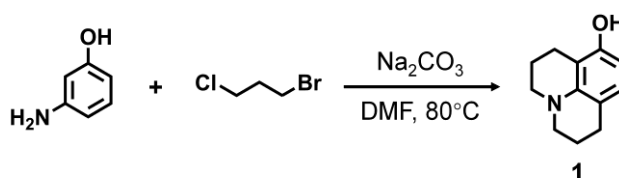


Figure S16. (A) Representative confocal fluorescence images from fixed HepG2 cells stained with **ROKS** (30 μ M, 10 min) (a) and incubated with PhSH (100 μ M, 10 min) (b), and then treated with HOCl (100 μ M, 10 min) (c). (B) Average fluorescence intensity in the green channel and the red channel from parallel images including (A). (C) Average fluorescence ratio ($I_{\text{Red}}/I_{\text{Green}}$) from parallel images including (A). Scale bar: 25 μ m. Green channel for PhSH: $\lambda_{\text{ex}} = 488$ nm, $\lambda_{\text{em}} = 500$ -550 nm; red channel for HOCl: $\lambda_{\text{ex}} = 561$ nm, $\lambda_{\text{em}} = 570$ -620 nm. Error bars are represented as the standard deviation (\pm S.D.) with $n = 3$. The number of dots represents that of samples. Significant differences (n.s., not significant, $**P < 0.01$, $***P < 0.001$) are analyzed with two-sided Student's t-test.

6. Synthetic methods

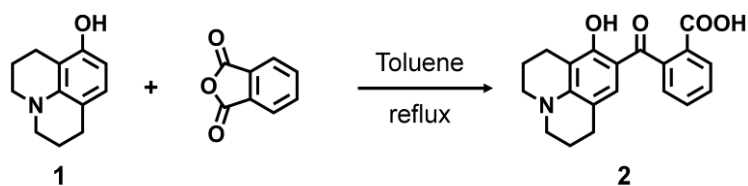
Synthesis of Compound 1



A mixture of *m*-aminophenol (2.18 g, 20 mmol), 1-Bromo-3-chloropropane (10 mL, 100 mmol) and anhydrous sodium carbonate (4.24 g, 40 mmol) was dissolved in *N,N*-dimethylformamide (15 mL). Under the protection of argon gas, the reaction mixture was

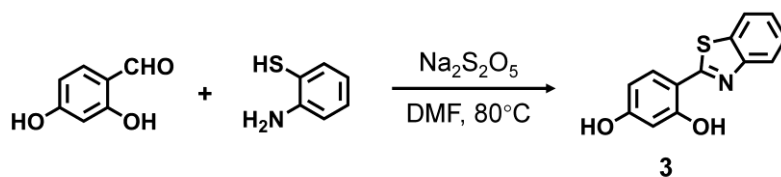
stirred at 80 °C for 15 h. After cooling, about 100 mL water was added and the resulting solution was extracted with dichloromethane (100 mL \times 3). The organic phase was dried with anhydrous MgSO_4 and evaporated under reduced pressure affording the crude product, which was further purified by chromatography using EA/PE (1:15, v/v) as eluent to afford compound **1** as a gray solid (2.62 g, 69%). Mp = 138-140 °C. ^1H NMR (400 MHz, CDCl_3) δ (ppm): 6.67 (d, J = 8.0 Hz, 1H), 6.06 (d, J = 8.0 Hz, 1H), 4.54 (s, 1H), 3.10 (q, J = 5.2 Hz, 4H), 2.72-2.65 (m, 4H), 2.03-1.93 (m, 4H); HRMS (ESI) m/z calcd for $\text{C}_{12}\text{H}_{16}\text{NO}$ $[\text{M}+\text{H}]^+$: 190.1226, found: 190.1222.

Synthesis of Compound 2



Compound **1** (2.84 g, 15 mmol) and *o*-phthalic anhydride (2.96 g, 20 mmol) in toluene (30 mL) was refluxed for 24 h. The solvent was evaporated under reduced pressure, and the residue was purified by chromatography using MeOH/DCM (1:40, v/v), and obtained compound **2** as a light green solid (2.33 g, 46%). Mp = 188-190 °C. ^1H NMR (400 MHz, $\text{DMSO}-d_6$) δ (ppm): 13.01 (s, 1H), 12.94 (s, 1H), 7.96-7.93 (m, 1H), 7.69-7.64 (m, 1H), 7.59 (q, J = 7.4 Hz, 1H), 7.35-7.32 (m, 1H), 6.40 (d, J = 5.3 Hz, 1H), 3.25-3.21 (m, 4H), 2.58 (t, J = 6.1 Hz, 2H), 2.40 (t, J = 6.1 Hz, 2H), 1.87-1.82 (m, 2H), 1.78-1.73 (m, 2H); HRMS (ESI) m/z calcd for $\text{C}_{20}\text{H}_{20}\text{NO}_4$ $[\text{M}+\text{H}]^+$: 338.1387, found: 338.1403.

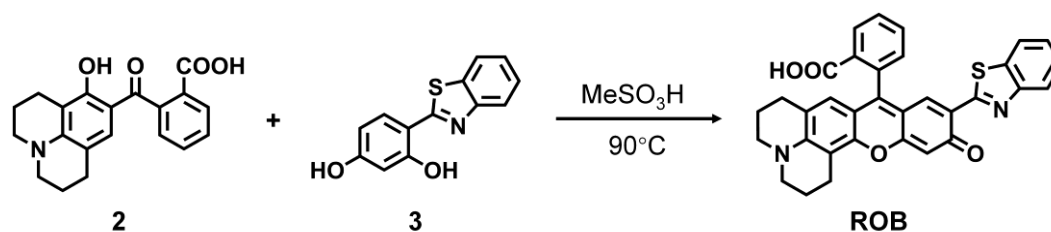
Synthesis of Compound 3



A mixture of 2,4-dihydroxybenzaldehyde (1.38 g, 10 mmol), *o*-amino thiophenol (1.07 mL, 10 mmol) and sodium metabisulfite (1.90 g, 10 mmol) was dissolved in *N,N*-dimethylformamide (30 mL) and the reaction solution was heated under reflux for 2 h with vigorous stirring. The reaction mixture was cooled to room temperature and then was added dropwise into water (100 mL). The precipitate was filtered, washed with water (10 mL \times 3), and then dried to give compound **3** as a yellow solid (1.83 g, 61%). Mp = 205-206 °C. ^1H NMR (600 MHz, $\text{DMSO}-d_6$) δ (ppm): 11.68 (s, 1H), 10.19 (s, 1H), 8.07 (d, J = 7.8 Hz, 1H),

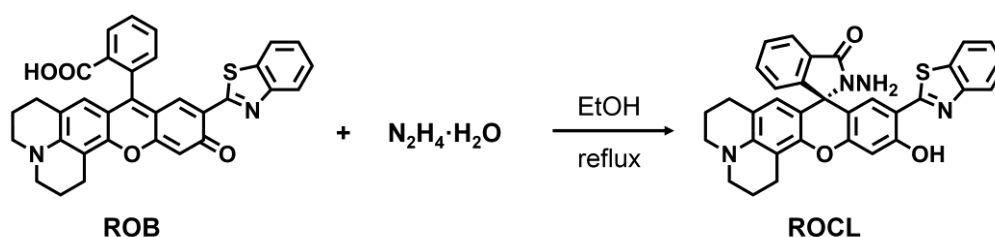
7.96 (d, $J = 8.0$ Hz, 1H), 7.92 (d, $J = 9.1$ Hz, 1H), 7.49 (t, $J = 7.5$ Hz, 1H), 7.38 (t, $J = 7.4$ Hz, 1H), 6.46 (s, 2H); HRMS (ESI) m/z calcd for $C_{13}H_{10}NO_2S$ $[M+H]^+$: 244.0435, found: 244.0439.

Synthesis of Compound ROB



A mixture of **2** (0.34 g, 1 mmol) and **3** (0.37 g, 1.5 mmol) in methanesulfonic acid (5 mL) was heated to 90 °C for 24 h under argon protection. After cooling, the reaction solution was poured into ice water (100 mL). The precipitate was filtered, and then washed with brine (10 mL \times 3) and ethyl ether (10 mL \times 3), and purified by chromatography using MeOH/DCM (1:30, v/v) to afford **ROB** as a purple solid (0.30 g, 56%). Mp > 250 °C. 1H NMR (400 MHz, DMSO- d_6 + drops of CF_3COOD) δ (ppm): 8.30 (d, $J = 7.7$ Hz, 1H), 8.06 (d, $J = 7.4$ Hz, 1H), 7.95-7.90 (m, 2H), 7.87-7.81 (m, 2H), 7.61 (d, $J = 7.3$ Hz, 1H), 7.44-7.36 (m, 2H), 7.28 (s, 1H), 6.46 (s, 1H), 3.65-3.56 (m, 4H), 2.95 (s, 2H), 2.48 (s, 2H), 2.10-1.98 (m, 2H), 1.79-1.73 (m, 2H); HRMS (ESI) m/z calcd for $C_{33}H_{25}N_2O_4S$ $[M+H]^+$: 545.1530, found: 545.1552; FT-IR (KBr, cm^{-1}): 3415.78, 2929.75, 2850.67, 1755.15, 1616.28, 1448.48, 1276.82, 1197.74, 1099.38, 854.43, 761.58, 713.63.

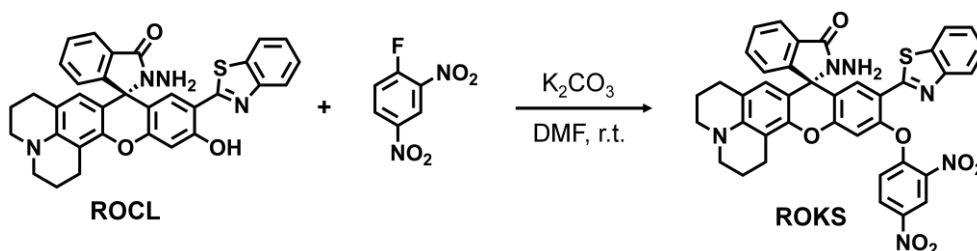
Synthesis of Compound ROCL



A solution of **ROB** (0.54 g, 1 mmol) in ethanol (30 mL) was added slowly hydrazine monohydrate (20 mL, 80%) and then the mixture was refluxed. After reaction for 5 h, the solvent was removed under reduced pressure. To the resulting residue was purified by chromatography using MeOH/DCM (1:200, v/v) to give **ROCL** as a gray solid (0.24 g, 42%). Mp > 250 °C. 1H NMR (400 MHz, DMSO- d_6) δ (ppm): 11.77 (s, 1H), 8.04 (d, $J = 7.8$ Hz, 1H), 7.93 (d, $J = 8.1$ Hz, 1H), 7.86-7.84 (m, 1H), 7.53-7.51 (m, 3H), 7.44 (t, $J = 7.4$ Hz, 1H), 7.36 (d, $J = 7.5$ Hz, 1H), 7.07-7.06 (m, 1H), 6.89 (s, 1H), 5.95 (s, 1H), 4.50 (s, 2H), 3.12-3.07

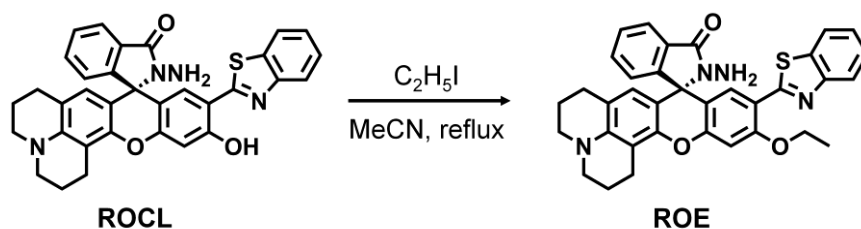
(m, 4H), 2.86 (t, $J = 6.0$ Hz, 2H), 2.47-2.37 (m, 2H), 1.95 (s, 2H), 1.77 (s, 2H); ^{13}C NMR (100 MHz, CDCl_3) δ : 168.41, 166.48, 159.15, 155.79, 151.68, 151.29, 148.29, 144.05, 133.03, 132.33, 129.71, 128.70, 127.85, 126.77, 125.57, 123.91, 123.81, 123.41, 122.02, 121.55, 118.37, 114.10, 111.62, 108.14, 104.92, 104.23, 65.83, 49.99, 49.53, 27.38, 21.90, 21.33, 21.25; HRMS (ESI) m/z calcd for $\text{C}_{33}\text{H}_{27}\text{N}_4\text{O}_3\text{S}$ $[\text{M}+\text{H}]^+$: 559.1798, found: 559.1742; FT-IR (KBr, cm^{-1}): 3425.43, 2927.82, 2842.95, 1697.28, 1610.49, 1498.63, 1431.12, 1307.68, 1168.81, 935.44, 711.70.

Synthesis of Compound ROKS



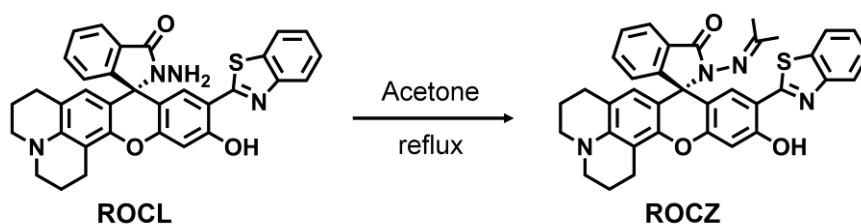
ROCL (0.56 g, 1 mmol), K_2CO_3 (0.14 g, 1 mmol) and 1-fluoro-2,4-dinitrobenzene (0.28 g, 1.5 mmol) were added to DMF (10 mL) and the mixture was stirred for 2 h at room temperature. After the reaction was complete, the resulting reaction mixture was poured into ice water. The precipitate was collected by filtration, and then purified by chromatography using MeOH/DCM (1:80, v/v) to give **ROKS** as a pale yellow solid (0.41 g, 57%). Mp > 250 °C. ^1H NMR (400 MHz, CDCl_3) δ (ppm): 8.88 (d, $J = 2.8$ Hz, 1H), 8.26 (dd, $J = 2.6, 9.2$ Hz, 1H), 7.98-7.96 (m, 1H), 7.86 (d, $J = 8.4$ Hz, 2H), 7.72 (d, $J = 8.0$ Hz, 1H), 7.49-7.47 (m, 2H), 7.36 (t, $J = 7.3$ Hz, 1H), 7.28-7.24 (m, 1H), 7.15-7.11 (m, 3H), 6.08 (s, 1H), 3.16-3.10 (m, 4H), 2.89 (t, $J = 6.5$ Hz, 2H), 2.54-2.49 (m, 2H), 2.01-1.98 (m, 2H), 1.88-1.84 (m, 2H); ^{13}C NMR (100 MHz, CDCl_3) δ : 167.08, 160.02, 155.07, 155.03, 152.55, 151.47, 151.14, 147.76, 143.91, 142.39, 139.96, 135.45, 135.37, 133.27, 130.75, 129.28, 129.19, 129.00, 126.56, 125.57, 123.79, 123.70, 123.41, 122.35, 122.00, 121.42, 119.43, 119.17, 119.13, 118.90, 110.09, 65.97, 65.57, 50.04, 49.54, 27.39, 21.76, 21.24, 15.40; HRMS (ESI) m/z calcd for $\text{C}_{39}\text{H}_{28}\text{NaN}_6\text{O}_7\text{S}$ $[\text{M}+\text{Na}]^+$: 747.1632, found: 747.1635; FT-IR (KBr, cm^{-1}): 3423.50, 3107.19, 3045.47, 2933.60, 2839.09, 2356.91, 1701.14, 1608.56, 1533.34, 1454.26, 1348.18, 1307.68, 1263.32, 1161.10, 916.15, 730.99.

Synthesis of Compound ROE



Under an argon atmosphere, **ROCL** (0.28 g, 0.5 mmol), K_2CO_3 (0.07 g, 0.5 mmol) and Iodoethane (44 μL , 0.55 mmol) were mixed in acetonitrile (10 mL) and the solution was refluxed for 16 h. The reaction solvent was evaporated off under reduced pressure to afford pale yellow, which was purified by chromatography using MeOH/DCM (1:100, v/v) to obtain **ROE** as a white solid (0.29 g, 75%). Mp > 250 °C. ^1H NMR (400 MHz, CDCl_3) δ (ppm): 8.00 (d, $J = 8.2$ Hz, 1H), 7.96 (d, $J = 8.1$ Hz, 1H), 7.91 (s, 1H), 7.85 (d, $J = 7.6$ Hz, 1H), 7.47-7.39 (m, 3H), 7.30 (t, $J = 8.1$ Hz, 1H), 7.08 (d, $J = 6.3$ Hz, 1H), 6.87 (s, 1H), 6.06 (s, 1H), 4.33 (q, $J = 7.2$ Hz, 2H), 3.85 (s, 2H), 3.16 (t, $J = 5.5$ Hz, 2H), 3.11 (t, $J = 5.5$ Hz, 2H), 2.96 (t, $J = 6.6$ Hz, 2H), 2.59-2.45 (m, 2H), 2.07-2.01 (m, 2H), 1.90-1.84 (m, 2H), 1.66 (t, $J = 6.9$ Hz, 3H); ^{13}C NMR (100 MHz, CDCl_3) δ : 167.01, 162.02, 157.38, 155.03, 151.97, 151.72, 148.07, 143.92, 135.85, 132.94, 129.39, 128.93, 128.50, 125.87, 124.43, 123.70, 123.66, 123.48, 122.77, 121.06, 118.89, 118.31, 111.87, 107.92, 104.77, 100.57, 65.86, 65.40, 49.95, 49.45, 27.35, 21.89, 21.36, 21.33, 14.88; HRMS (ESI) m/z calcd for $\text{C}_{35}\text{H}_{31}\text{N}_4\text{O}_3\text{S}$ $[\text{M}+\text{H}]^+$: 587.2111, found: 587.2097; FT-IR (KBr, cm^{-1}): 3440.80, 2937.40, 1687.61, 1610.46, 1421.45, 1307.65, 1184.22, 761.83.

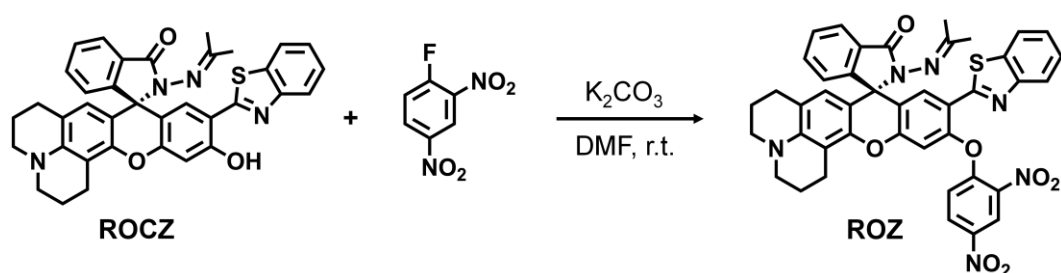
Synthesis of Compound ROCZ



ROCL (1.28 g, 2.3 mmol) were refluxed in acetone (15 mL) for 5 h. The reaction solvent was removed under vacuum, and the residue was then purified by chromatography using MeOH/DCM (1:100, v/v) to give **ROCZ** as a white solid (1.10 g, 80%). Mp > 250 °C. ^1H NMR (400 MHz, CDCl_3) δ (ppm): 7.98-7.96 (m, 1H), 7.89 (d, $J = 4.8$ Hz, 1H), 7.76 (d, $J = 7.9$ Hz, 1H), 7.53-7.49 (m, 2H), 7.46-7.42 (m, 1H), 7.33 (t, $J = 7.6$ Hz, 1H), 7.14 (d, $J = 6.6$ Hz, 1H), 7.04 (s, 1H), 6.87 (s, 1H), 6.16 (s, 1H), 3.17-3.10 (m, 4H), 2.93 (t, $J = 6.7$ Hz, 2H), 2.57-2.47 (m, 2H), 2.05-2.02 (m, 2H), 1.98 (s, 3H), 1.88 (s, 5H); ^{13}C NMR (100 MHz, CDCl_3) δ : 174.30, 168.65, 160.92, 158.78, 155.71, 151.75, 151.48, 148.00, 143.73, 132.62,

132.25, 130.30, 128.59, 128.24, 126.71, 125.45, 124.45, 123.74, 123.36, 121.95, 121.47, 117.86, 113.63, 112.98, 107.84, 105.95, 104.57, 66.03, 49.97, 49.51, 27.36, 25.64, 21.97, 21.82, 21.41, 21.21; HRMS (ESI) m/z calcd for $C_{36}H_{31}N_4O_3S$ $[M+H]^+$: 599.2111, found: 599.2101; FT-IR (KBr, cm^{-1}): 3436.94, 2929.69, 1703.04, 1623.96, 1494.74, 1444.59, 1309.58, 1178.43, 756.05.

Synthesis of Compound ROZ



ROCZ (0.39 g, 0.65 mmol), K_2CO_3 (0.14 g, 1 mmol) and 2,4-dinitrofluorobenzene (84 μ L, 0.72 mmol) were added to DMF (10 mL) and the mixture was stirred for 2 h at room temperature. After the reaction was complete, the resulting reaction mixture was poured into ice water. The precipitate was collected by filtration and then purified by chromatography using MeOH/DCM (1:100, v/v) to give **ROZ** as a pale yellow solid (0.27 g, 47%). Mp > 250 $^{\circ}C$. 1H NMR (400 MHz, $CDCl_3$) δ (ppm): 8.92 (s, 1H), 8.30 (d, J = 6.4 Hz, 1H), 7.99 (d, J = 8.6 Hz, 1H), 7.87 (d, J = 11.1 Hz, 2H), 7.74 (d, J = 7.8 Hz, 1H), 7.54-7.51 (m, 2H), 7.40 (t, J = 7.7 Hz, 1H), 7.29 (t, J = 7.1 Hz, 1H), 7.16 (d, J = 5.4 Hz, 1H), 7.09 (t, J = 8.6 Hz, 2H), 6.21 (s, 1H), 3.17-3.12 (m, 4H), 2.89 (t, J = 6.4 Hz, 2H), 2.61-2.48 (m, 2H), 2.02 (s, 5H), 1.96 (s, 3H), 1.90-1.85 (m, 2H); HRMS (ESI) m/z calcd for $C_{42}H_{33}N_6O_7S$ $[M+H]^+$: 765.2126, found: 765.2101; FT-IR (KBr, cm^{-1}): 3448.51, 2923.90, 1701.11, 1614.32, 1535.24, 1446.52, 1305.72, 1168.79, 730.97.

7. Characterization of compounds

Table S2. Crystal data and structure refinement summary for **ROKS**, **ROCL** and **ROB**.

	ROKS	ROCL	ROB
Empirical formula	$C_{39}H_{28}N_6O_7S$	$C_{33}H_{26}N_4O_3S$	$C_{33}H_{24}N_2O_4S$
Formula weight	724.75	558.64	544.60
Temperature/K	296	296	296
Crystal system	monoclinic	triclinic	triclinic
Space group	P 1 21/c 1	P-1	P-1
$a/\text{\AA}$	17.669(5)	10.077(2)	7.8981(18)

$b/\text{\AA}$	9.336(3)	10.691(2)	10.981(2)
$c/\text{\AA}$	23.887(7)	13.476(3)	15.616(4)
$\alpha/^\circ$	90	101.301(3)	72.196(4)
$\beta/^\circ$	102.697(6)	96.718(3)	88.661(4)
$\gamma/^\circ$	90	105.176(3)	80.402(4)
Volume/ \AA^3	3844.3(19)	1352.1(4)	1270.9(5)
Z	4	2	2
$\rho_{\text{calc}} \text{ g/cm}^3$	1.380	1.372	1.423
μ/mm^{-1}	0.149	0.163	0.172
$F(000)$	1672.0	584	568
$h_{\text{min,max}}$	-20, 21	-12, 9	-9, 9
$k_{\text{min,max}}$	-11, 11	-12, 11	-12, 13
$l_{\text{min,max}}$	-18, 29	-16, 16	-19, 17
No. of Reflns.	20245/7633	7038/4942	6981/4981
R_{int}	0.0811	0.0198	0.0239
GOF on F^2	0.982	1.014	1.021
$R_1^a [I > 2\sigma(I)]$	0.0740	0.0567	0.0529
wR_2^b (all data)	0.2298	0.1683	0.1375
CCDC	2018843	2018838	2018837

Table S3. Crystal data and structure refinement summary for **ROE**, **ROCZ** and **ROZ**.

	ROE	ROCZ	ROZ
Empirical formula	$\text{C}_{35}\text{H}_{30}\text{N}_4\text{O}_3\text{S}$	$\text{C}_{36}\text{H}_{30}\text{N}_4\text{O}_3\text{S}$	$\text{C}_{42}\text{H}_{32}\text{N}_6\text{O}_7\text{S}$
Formula weight	586.69	598.20	764.79
Temperature/K	296	296	174
Crystal system	monoclinic	monoclinic	monoclinic
Space group	C 1 2/c 1	C 1 2/c 1	P 1 21/c 1
$a/\text{\AA}$	23.381(7)	32.58(3)	17.642(3)
$b/\text{\AA}$	19.573(7)	12.432(11)	9.1727(18)
$c/\text{\AA}$	15.988(5)	16.118(15)	23.263(5)

$\alpha/^\circ$	90	90	90
$\beta/^\circ$	117.634(9) $^\circ$	94.57(2)	101.185(9)
$\gamma/^\circ$	90	90	90
Volume/ \AA^3	6482(4)	6508(10)	3693.0(13)
Z	8	8	4
$\rho_{\text{calc}} \text{ g/cm}^3$	1.235	1.309	1.376
μ/mm^{-1}	0.143	0.224	0.837
$F(000)$	2528.0	2680.0	1592.0
$h_{\text{min,max}}$	-27, 27	-21, 38	-19, 21
$k_{\text{min,max}}$	-21, 23	-14, 14	-11, 11
$l_{\text{min,max}}$	-19, 16	-19, 17	-28, 28
No. of Reflins.	15991/5714	14140/5725	31566/6969
R_{int}	0.1629	0.1635	0.0547
GOF on F^2	0.903	0.957	1.049
$R_1^{\text{a}} [I > 2\sigma(I)]$	0.0975	0.0994	0.0759
wR_2^{b} (all data)	0.3382	0.2962	0.2599
CCDC	2018842	2018841	2018844

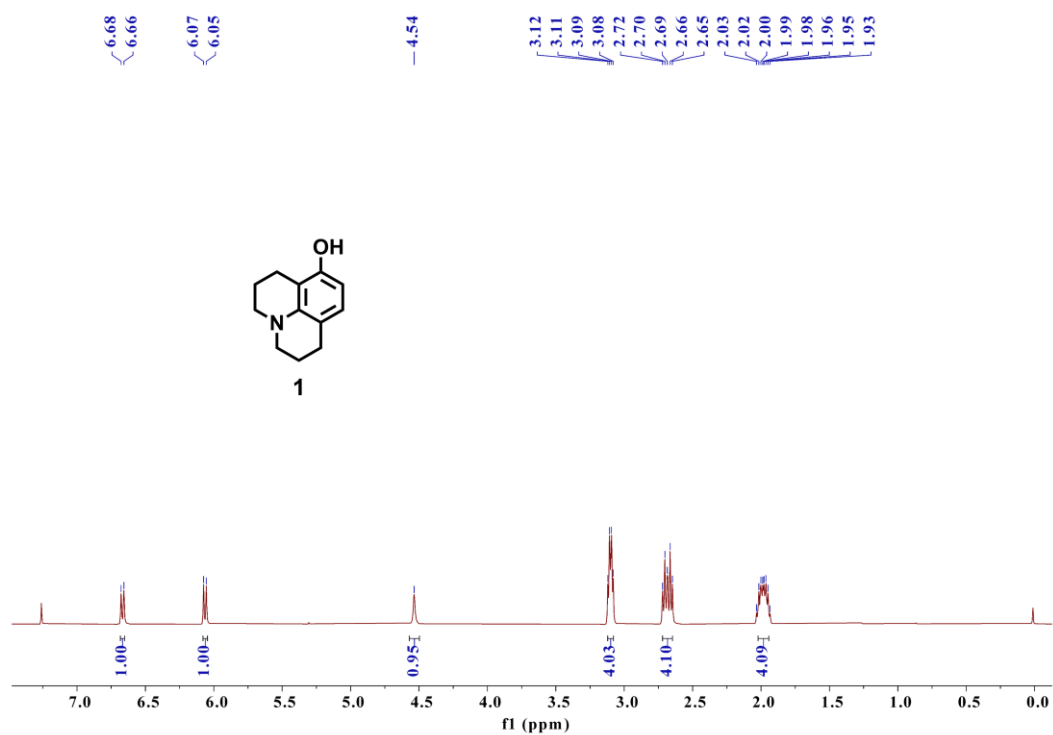


Figure S17. ¹H NMR spectrum of compound **1** in CDCl₃.

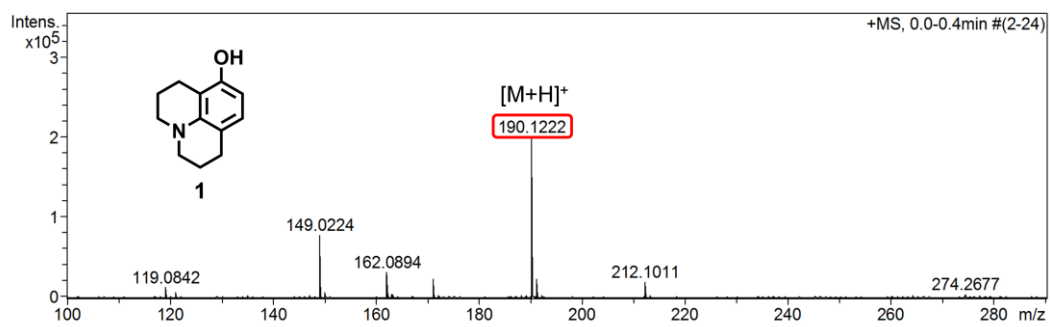


Figure S18. HRMS spectrum of compound **1**.

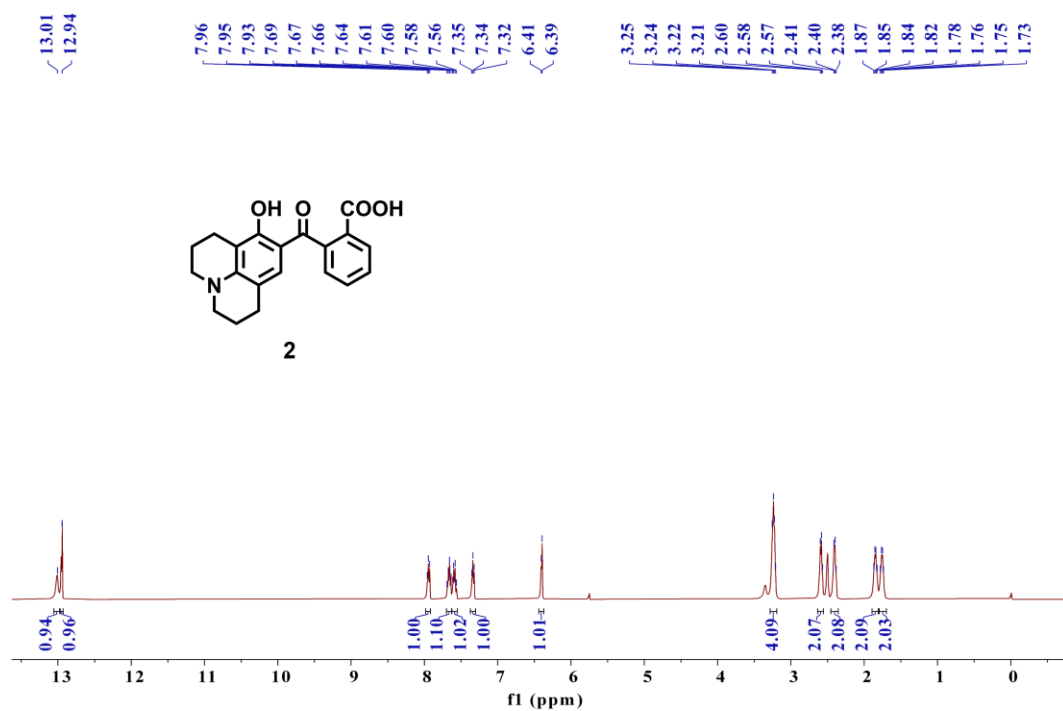


Figure S19. ¹H NMR spectrum of compound **2** in DMSO-*d*₆.

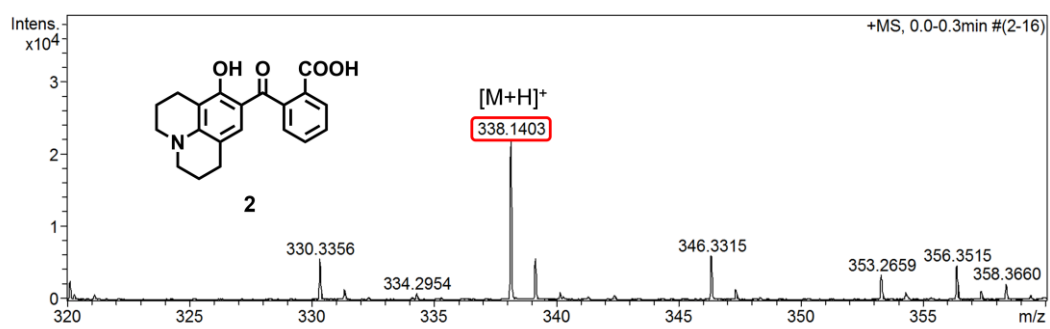


Figure S20. HRMS spectrum of compound **2**.

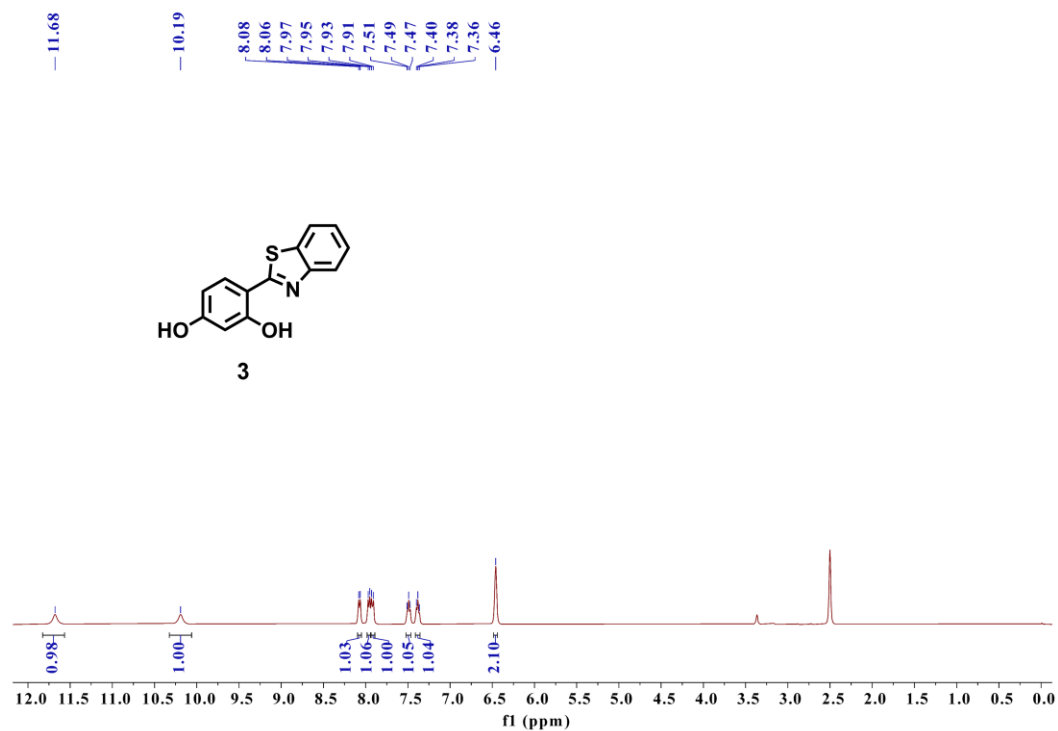


Figure S21. ¹H NMR spectrum of compound **3** in DMSO-*d*₆.

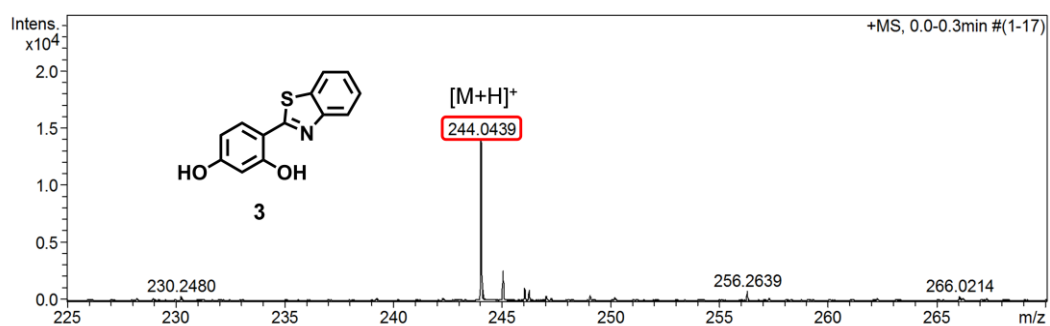


Figure S22. HRMS spectrum of compound **3**.

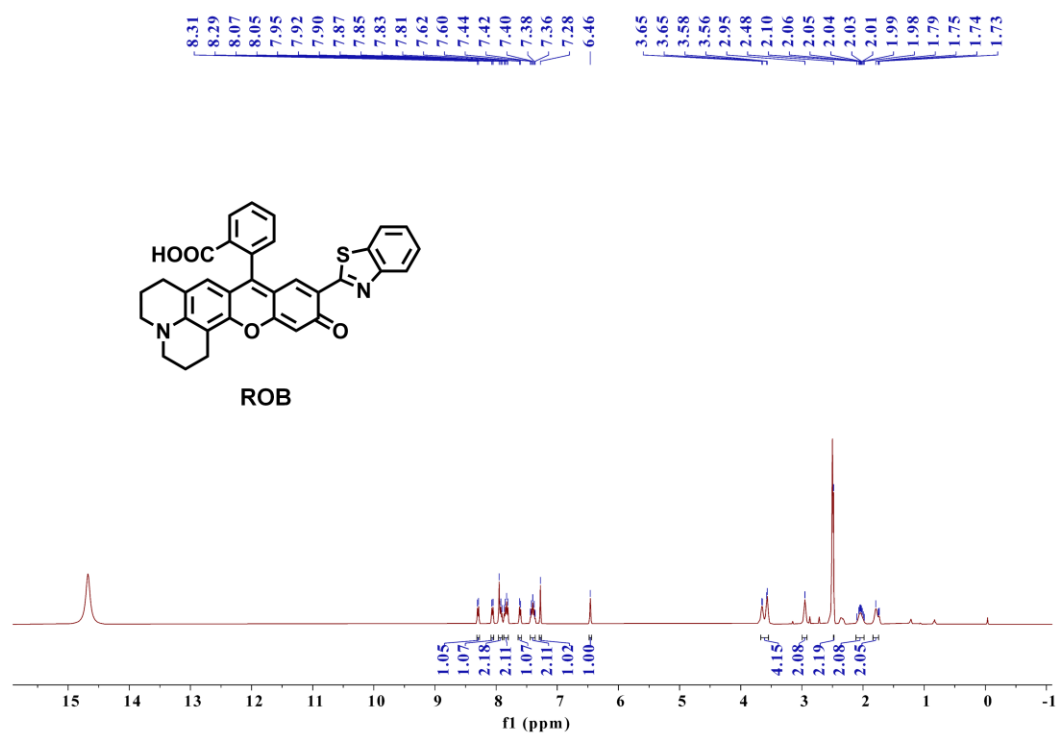


Figure S23. ^1H NMR spectrum of compound **ROB** in $\text{DMSO}-d_6$ + drops of CF_3COOD .

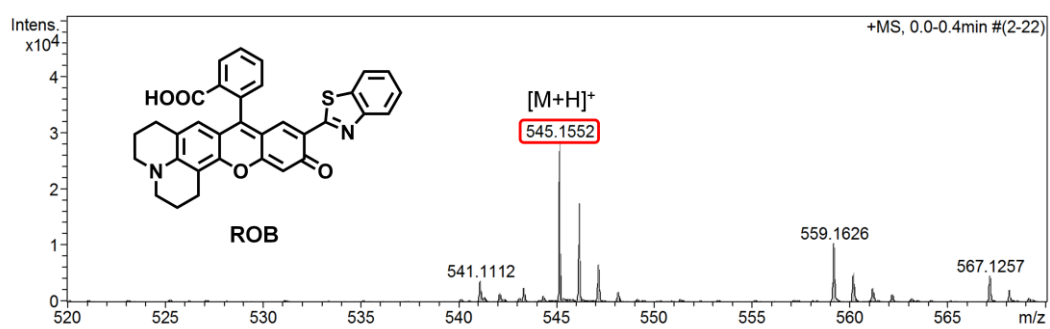


Figure S24. HRMS spectrum of compound **ROB**.

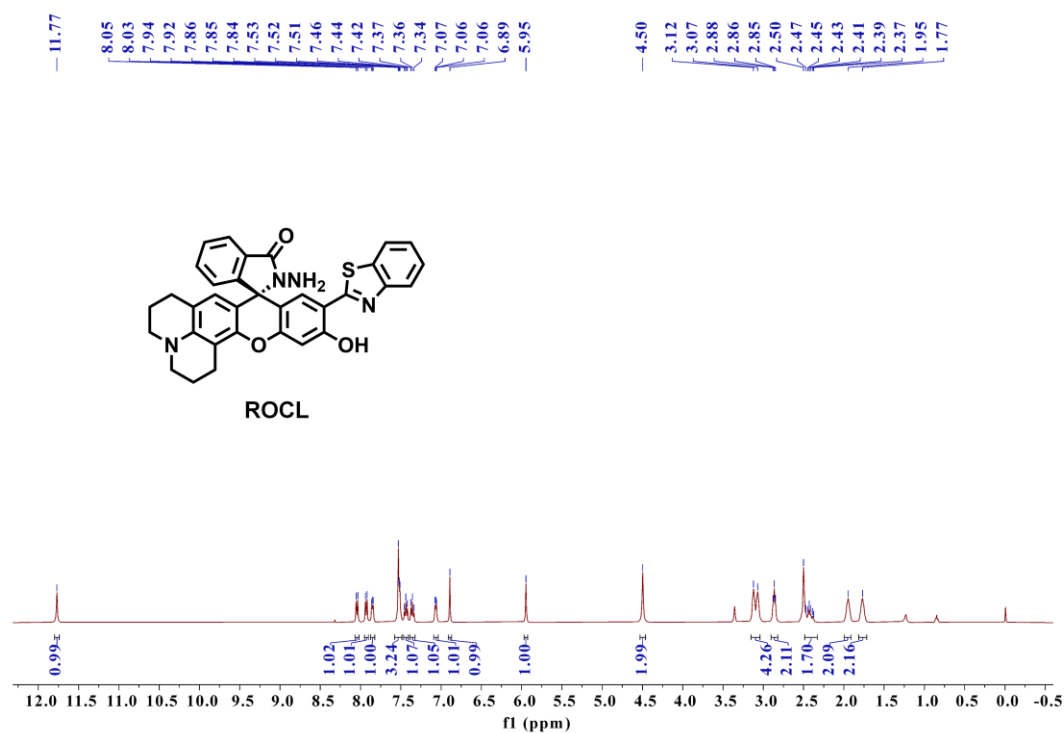


Figure S25. ¹H NMR spectrum of compound **ROCL** in DMSO-*d*₆.

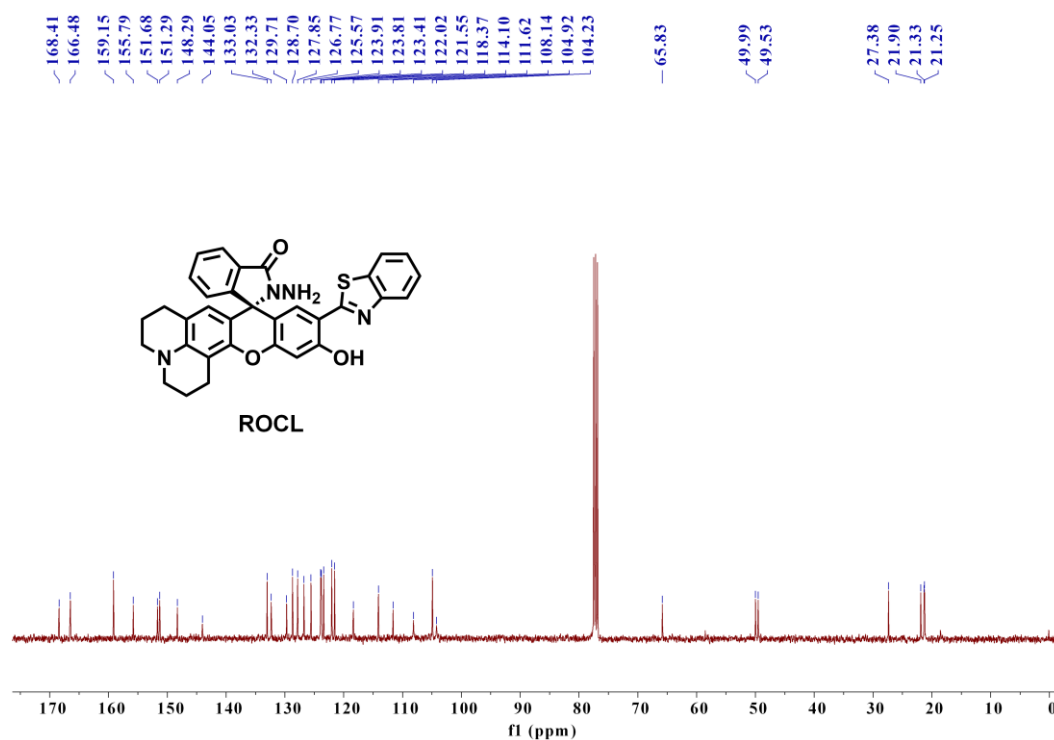


Figure S26. ¹³C NMR spectrum of compound **ROCL** in CDCl₃.

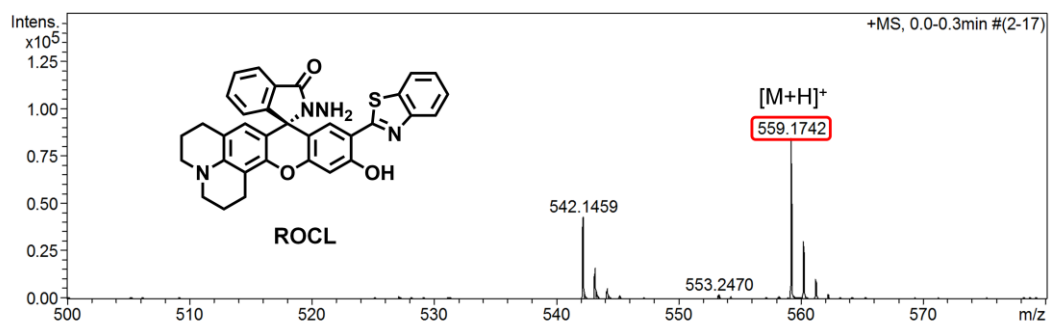


Figure S27. HRMS spectrum of compound **ROCL**.

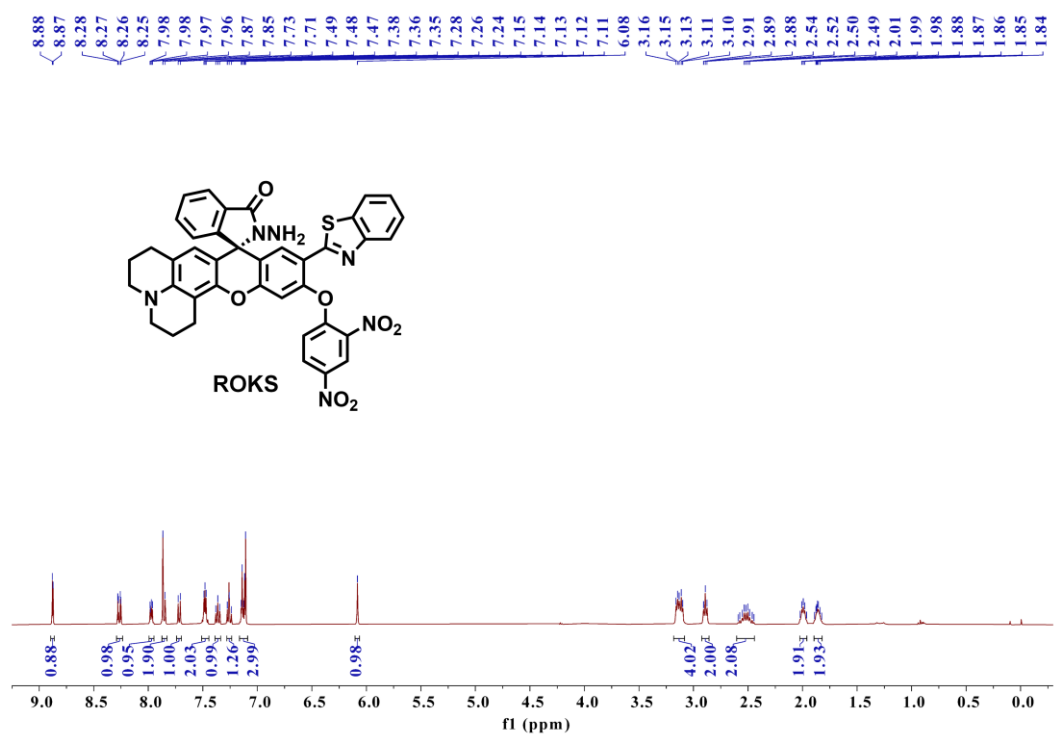


Figure S28. ¹H NMR spectrum of compound **ROKS** in CDCl₃.

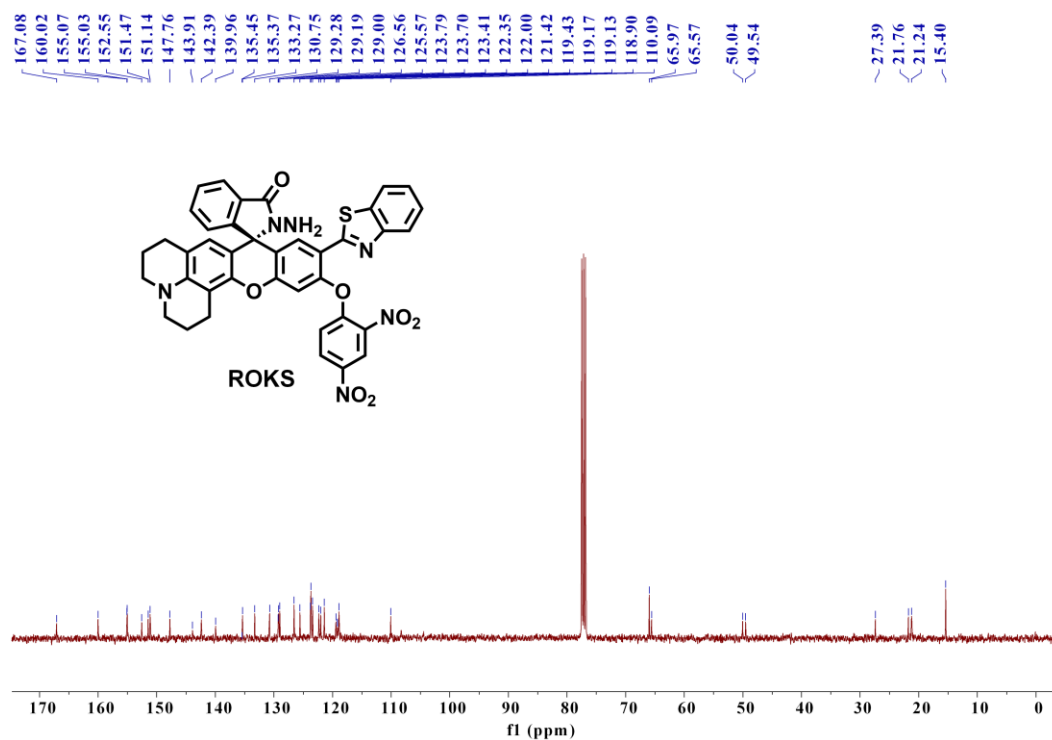


Figure S29. ¹³C NMR spectrum of compound **ROKS** in CDCl₃.

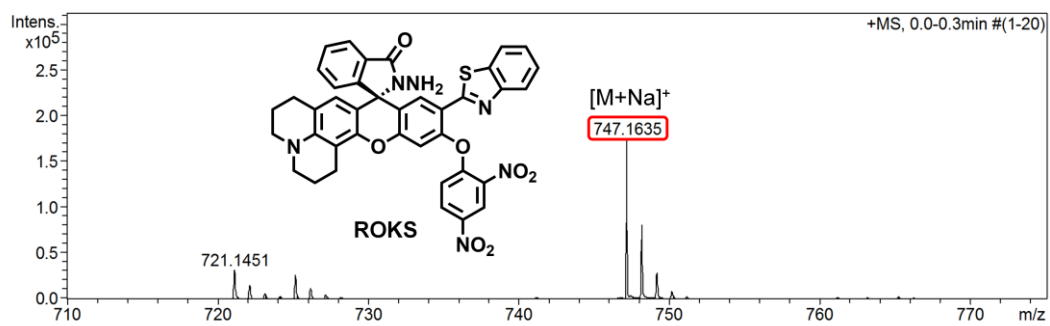


Figure S30. HRMS spectrum of compound **ROKS**.

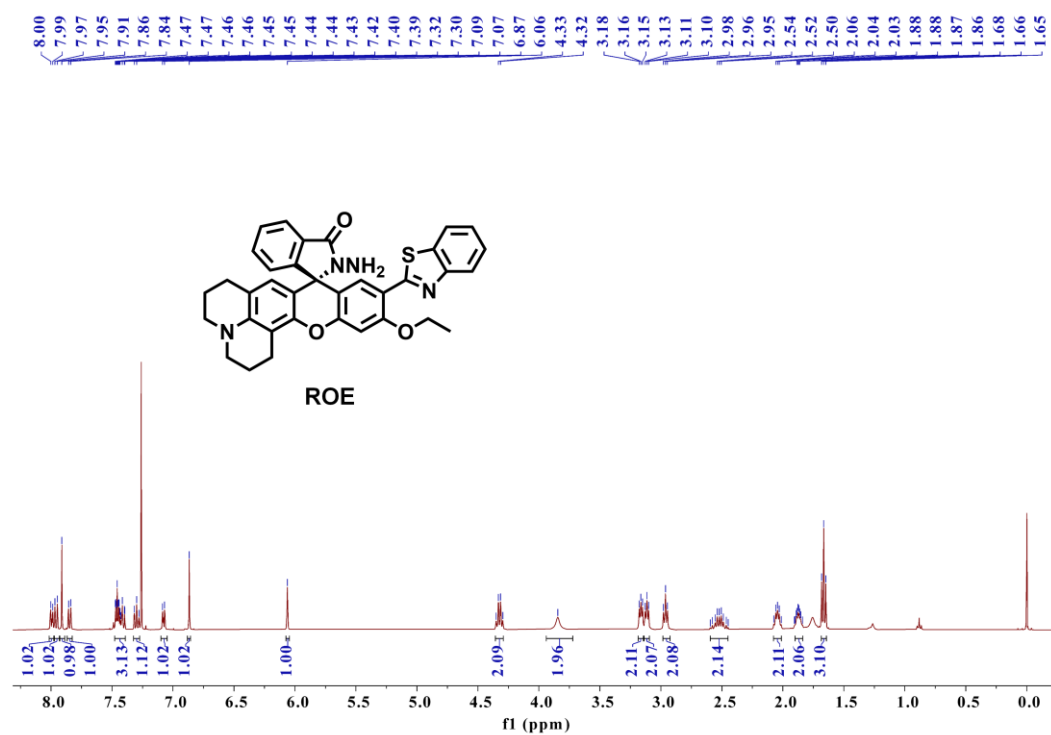


Figure S31. ^1H NMR spectrum of compound **ROE** in CDCl_3 .

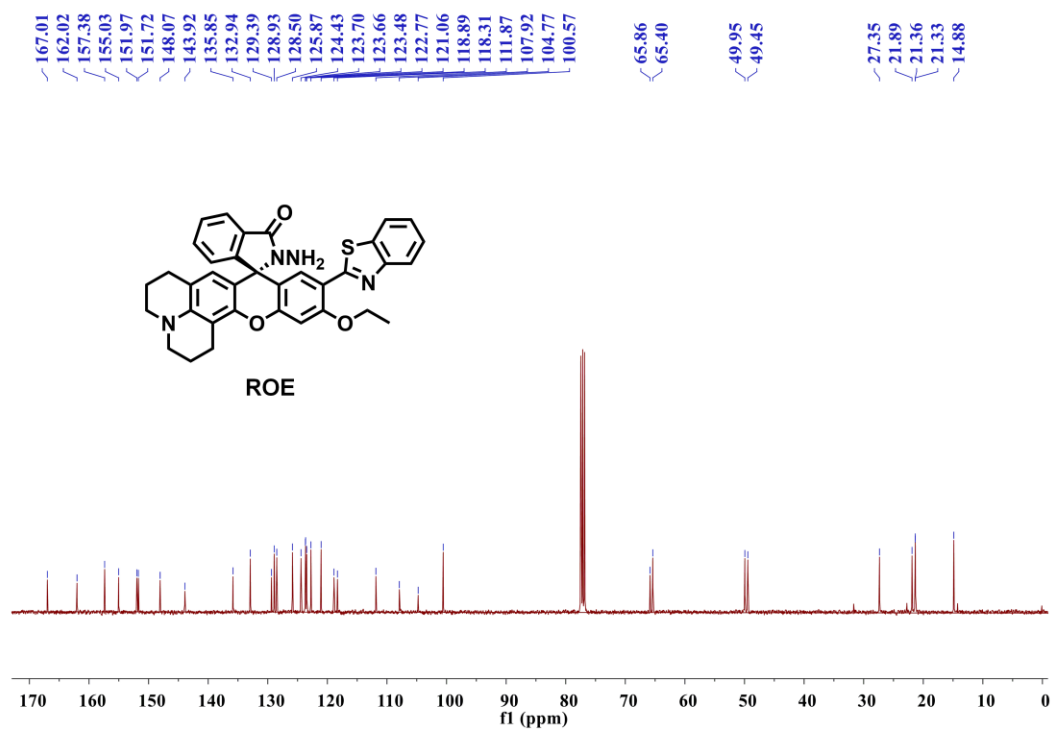


Figure S32. ^{13}C NMR spectrum of compound **ROE** in CDCl_3 .

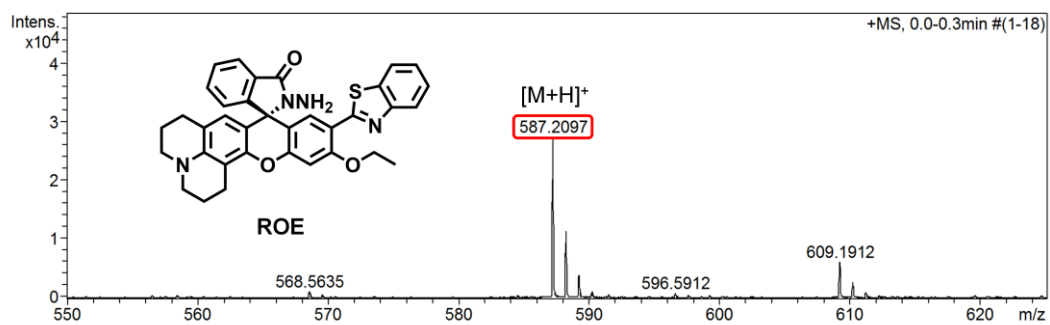


Figure S33. HRMS spectrum of compound **ROE**.

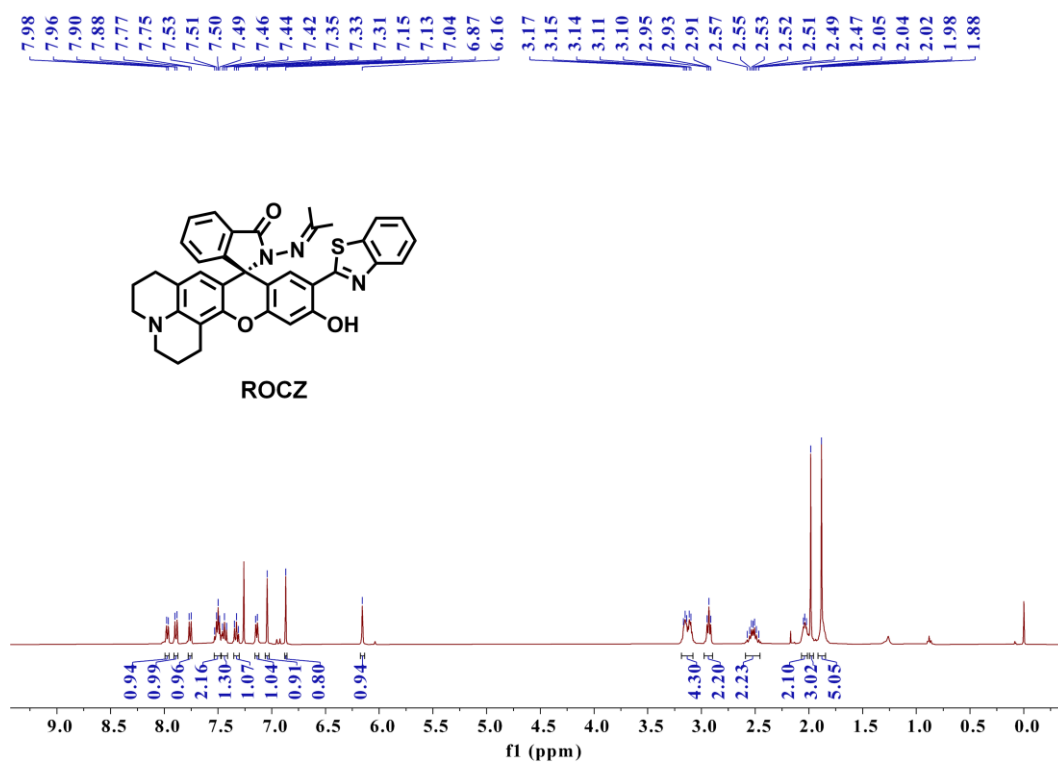


Figure S34. ¹H NMR spectrum of compound **ROCZ** in CDCl₃.

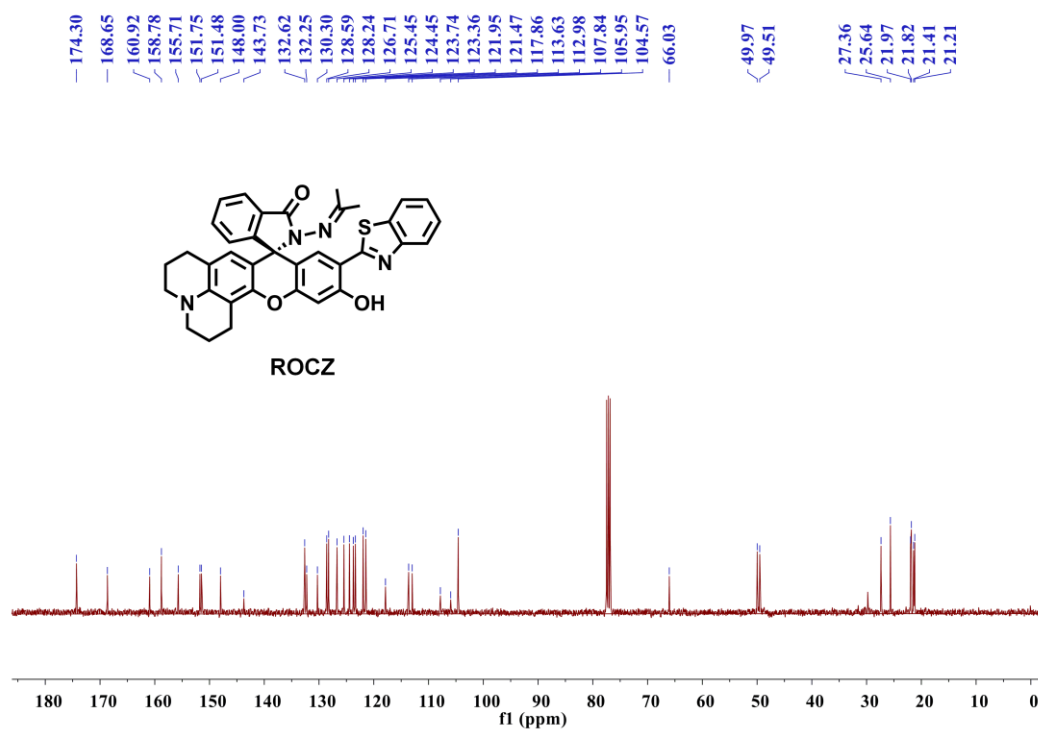


Figure S35. ¹³C NMR spectrum of compound **ROCZ** in CDCl₃.

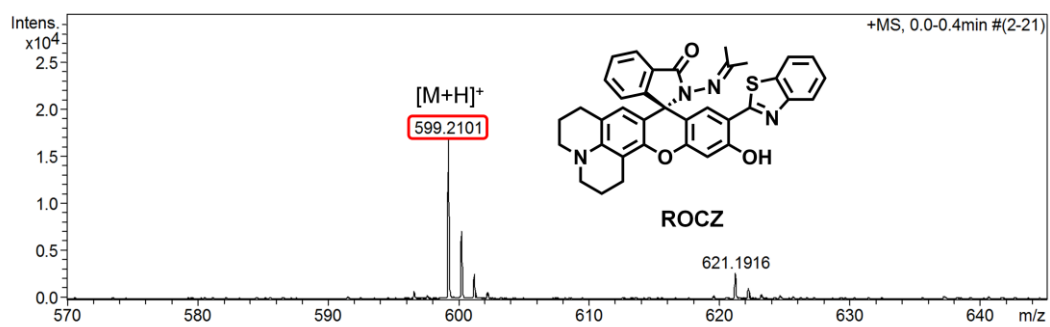


Figure S36. HRMS spectrum of compound **ROCZ**.

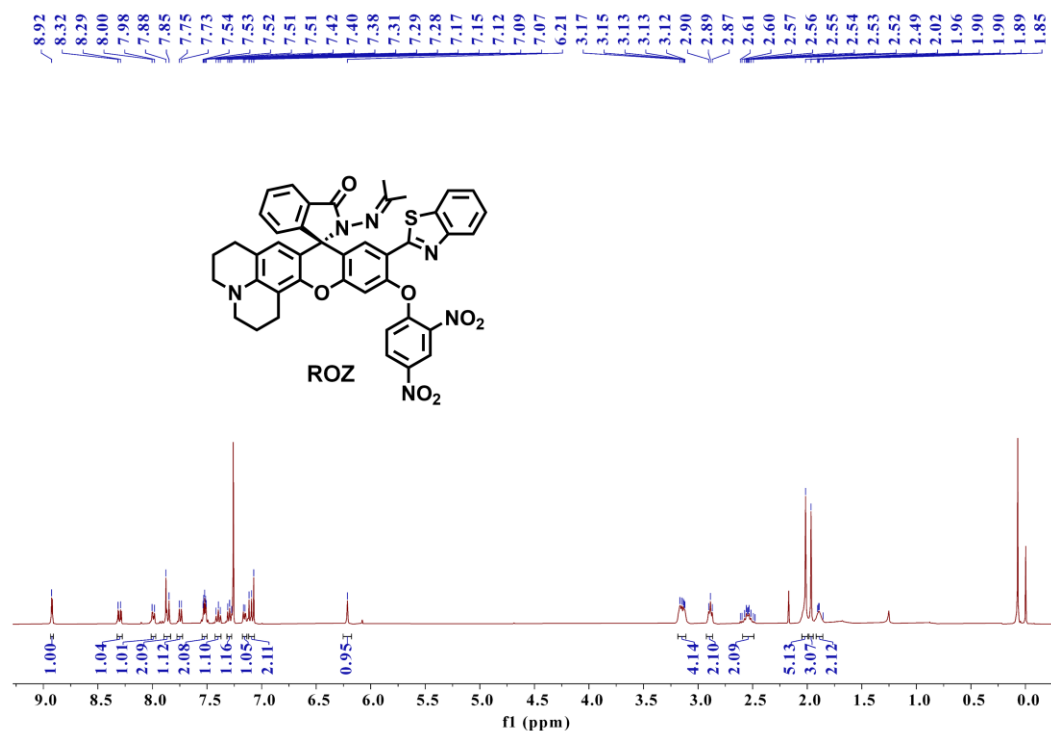


Figure S37. ^1H NMR spectrum of compound **ROZ** in CDCl_3 .

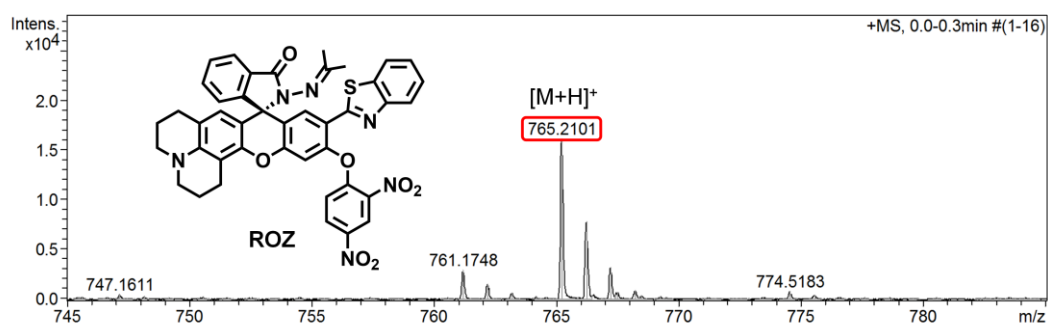


Figure S38. HRMS spectrum of compound **ROZ**.

References

1. C. B. Hübschle, G. M. Sheldrick and B. Dittrich, *J. Appl. Cryst.*, 2011, **44**, 1281-1284.
2. S. Devi and D. Jananakumar, *Chin. J. Phys.*, 2020, **68**, 339-347.
3. G. W. Chen, F. L. Song, J. Y. Wang, Z. G. Yang, S. G. Sun, J. L. Fan, X. X. Qiang, X. Wang, B. R. Dou and X. J. Peng, *Chem. Commun.*, 2012, **48**, 2949-2951.

4. A. C. Sedgwick, W. T. Dou, J. B. Jiao, L. L. Wu, G. T. Williams, A. T. A. Jenkins, S. D. Bull, J. L. Sessler, X. P. He and T. D. James, *J. Am. Chem. Soc.*, 2018, **140**, 14267-14271.
5. G. Weber and F. W. J. Teale, *Trans. Faraday Soc.*, 1957, **53**, 646-655.
6. H. B. Xiao, X. Liu, C. C. Wu, Y. H. Wu, P. Li, X. M. Guo and B. Tang, *Biosens. Bioelectron.*, 2017, **91**, 449-455.
7. J. D. Chai and M. Head-Gordon, *Phys. Chem. Chem. Phys.*, 2008, **10**, 6615-6620.
8. M. J. Frisch, G. W. Trucks, H. B. Schlegel, G. E. Scuseria, M. A. Robb, J. R. Cheeseman, G. Scalmani, V. Barone, B. Mennucci, G. A. Petersson, H. Nakatsuji, M. Caricato, X. Li, H. P. Hratchian, A. F. Izmaylov, J. Bloino, G. Zheng, J. L. Sonnenberg, M. Hada, M. Ehara, K. Toyota, R. Fukuda, J. Hasegawa, M. Ishida, T. Nakajima, Y. Honda, O. Kitao, H. Nakai, T. Vreven, Jr. J. A. Montgomery, J. E. Peralta, F. Ogliaro, M. Bearpark, J. J. Heyd, E. Brothers, K. N. Kudin, V. N. Staroverov, R. Kobayashi, J. Normand, K. Raghavachari, A. Rendell, J. C. Burant, S. S. Iyengar, J. Tomasi, M. Cossi, N. Rega, J. M. Millam, M. Klene, J. E. Knox, J. B. Cross, V. Bakken, C. Adamo, J. Jaramillo, R. Gomperts, R. E. Stratmann, O. Yazyev, A. J. Austin, R. Cammi, C. Pomelli, J. W. Ochterski, R. L. Martin, K. Morokuma, V. G. Zakrzewski, G. A. Voth, P. Salvador, J. J. Dannenberg, S. Dapprich, A. D. Daniels, O. Farkas, J. B. Foresman, J. V. Ortiz, J. Cioslowski and D. J. Fox, Gaussian 09, revision D.01; Gaussian, Inc.: Wallingford, CT, 2013.
9. X. K. Li, W. J. Qiu, J. W. Li, X. Chen, Y. L. Hu, Y. Gao, D. L. Shi, X. M. Li, H. L. Lin, Z. L. Hu, G. Q. Dong, C. Q. Sheng, B. Jiang, C. L. Xia, C. Y. Kim, Y. Guo and J. Li, *Chem. Sci.*, 2020, **11**, 7292-7301.